British Journal of Pharmacology (2003) 139, 733–740
www.nature.com/bjp

Role of PAF receptors during intestinal ischemia and reperfusion injury. A comparative study between PAF receptor-deficient mice and PAF receptor antagonist treatment

[1]Danielle G. Souza, [1]Vanessa Pinho, [1]Adriana C. Soares, [2,3]Takao Shimizu, [2,3]Satoshi Ishii & *,[1]Mauro M. Teixeira

[1]Departamento de Bioquímica e Imunologia, Instituto de Ciências Biológicas, Universidade Federal de Minas Gerais, Belo Horizonte, Brazil; [2]Department of Biochemistry and Molecular Biology, Faculty of Medicine, The University of Tokyo, Japan and [3]CREST of Japan Science and Technology Corporation, Tokyo, Japan

1 The reperfusion of ischemic tissues may be associated with local and systemic inflammation that prevents the full benefit of blood flow restoration. The present study aimed to confirm a role for platelet-activating factor receptor(s) (PAFR) during ischemia and reperfusion injury by using genetically modified mice deficient in the PAFR ($PAFR^{-/-}$ mice) and to evaluate comparatively the effectiveness of pharmacological treatment using the PAFR antagonist UK-74,505 (modipafant).

2 The reperfusion of the ischemic superior mesenteric artery (SMA) induced marked local (intestine) and remote (lungs) tissue injury, as assessed by the increase in vascular permeability, neutrophil influx and intestinal hemorrhage and in the production of TNF-α. There was also a systemic inflammatory response, as shown by the increase in serum TNF-α concentrations and marked reperfusion-associated lethality.

3 After reperfusion of the ischemic SMA, $PAFR^{-/-}$ mice had little tissue or systemic inflammation and lethality was delayed, but not prevented, in these mice. Interestingly, the reperfusion-associated increases in tissue concentrations of IL-10 were significantly greater in $PAFR^{-/-}$ than wild-type mice.

4 Pretreatment with PAFR antagonist UK-74,505 (1 mg kg^{-1}) markedly prevented tissue injury, as assessed by the increase in vascular permeability, neutrophil accumulation, hemorrhage and TNF-α concentrations in the intestine and lungs. In contrast, UK-74,505 failed to affect reperfusion-associated lethality and increases in serum TNF-α when used at 1 mg kg^{-1}.

5 Reperfusion-associated lethality and increase in serum TNF-α were only affected when a supra-maximal dose of the antagonist was used (10 mg kg^{-1}). At this dose, UK-74,505 also induced a marked enhancement of reperfusion-associated increases in tissue concentrations of IL-10. However, at the same dose, UK-74,505 failed to prevent reperfusion-associated lethality in $PAFR^{-/-}$ mice any further.

6 The present studies using genetically modified animals and a receptor antagonist firmly establish a role of PAFR activation for the local, remote and systemic inflammatory injury and lethality which follows reperfusion of the ischemic SMA in mice. Moreover, it is suggested that high doses of PAFR antagonists need to be used if the real efficacy of these compounds is to be tested clinically.

British Journal of Pharmacology (2003) **139**, 733–740. doi:10.1038/sj.bjp.0705296

Keywords: PAF receptor; lung injury; inflammation; TNF-α;IL-10

Abbreviations: I/R, ischemia and reperfusion; MPO, myeloperoxidase; PAF, platelet-activating factor; PAFR, platelet-activating factor receptor(s); $PAFR^{-/-}$ mice, platelet-activating factor receptor-deficient mice; SMA, superior mesenteric artery

Introduction

A major goal in the treatment of ischemia of a vascular territory is to restore blood flow to normal values, that is, to 'reperfuse' the ischemic vascular bed (Carden & Granger, 2000). However, reperfusion of ischemic tissues is associated with local and systemic leukocyte activation and trafficking, endothelial barrier dysfunction in postcapillary venules, enhanced production of inflammatory mediators and great lethality (Lefer & Lefer, 1996; Granger, 1999; Carden & Granger, 2000). For example, after intestinal ischemia and reperfusion (I/R), there is marked intestinal and pulmonary injury that may also be accompanied by a systemic inflammatory response syndrome and significant lethality (Souza *et al.*, 2000b; 2001; 2002). Among the mediators of the inflammatory cascade released and thought to be important for the reperfusion-associated injury is platelet-activation factor (PAF) (Kubes *et al.*, 1990a, b; Montrucchio *et al.*, 2000; Souza *et al.*, 2000b).

PAF is a natural phospholipid that under normal physiological conditions is minimally expressed. However, during acute inflammation or under conditions of oxidative stress, as occurs during I/R injury, PAF is released by neutrophils and/

*Author for correspondence at: Departamento de Bioquímica e Imunologia, Instituto de Ciencias Biologicas, Universidade Federal de Minas Gerais, Av. Antonio Carlos, 6627 Pampulha, 31270-901 Belo Horizonte MG, Brazil; E-mail: mmtex@icb.ufmg.br

or monocytes and expressed at the outer leaflet of endothelial cells (Montrucchio *et al.*, 2000). Once released, activation of PAF receptors (PAFR) results in diverse biological activities associated with acute inflammation, including neutrophil activation and chemotaxis, alterations in vascular permeability and platelet activation, all of which may contribute to the clinical manifestation of I/R injury (Montrucchio *et al.*, 2000).

We have recently described the effects of the treatment with the PAFR antagonists UK-74,505 and WEB-2086 in models of neutrophil-dependent mild and severe I/R injury in rats (Souza *et al.*, 2000b). Our results demonstrated that treatment with the PAFR antagonists prevented the increases in vascular permeability, neutrophil recruitment and TNF-α production (Souza *et al.*, 2000b). Furthermore, activation of PAFR has been shown to play an important pathophysiological role in models of I/R injury in several other vascular territories, including the heart, gut, kidney and lung (Canale *et al.*, 1994; Carter *et al.*, 1996; Riera *et al.*, 1997; Qayumi *et al.*, 1998; Morgan *et al.*, 1999; Kecskemeti & Balogh, 2000; Kim *et al.*, 2000; Sun *et al.*, 2001; 2002). The objectives of the present study were two-fold: (i) to confirm a role for PAFR during I/R injury by using genetically modified mice deficient in the PAFR ($PAFR^{-/-}$ mice); and (ii) to evaluate comparatively the effectiveness of pharmacological treatment using the PAFR antagonist UK-74,505 and the genetic PAFR deficiency.

Methods

Animals

Male C57BL/6 mice (8–10 weeks) obtained from the Bioscience unit of Instituto de Ciências Biológicas were housed under standard conditions and had free access to commercial chow and water. All procedures described here had prior approval from the local animal ethics committee. $PAFR^{-/-}$ mice were generated as previously described (Ishii *et al.*, 1998) and intercrossed for at least seven generations to establish the C57BL/6 strain.

Ischemia and reperfusion

Mice were anesthetized with urethane (140 mg kg^{-1}, i.p.) and laparotomy was performed. The superior mesenteric artery (SMA) was isolated and ischemia was induced by totally occluding the SMA for 60 min. For measuring the percentage of surviving mice, reperfusion was re-established, and mice were monitored for indicated time periods. For the other parameters, reperfusion was allowed to occur for 30 min (I60R30) when mice were killed. This time of reperfusion (30 min) was chosen based on the presence of significant tissue injury without unduly high mortality rates. Sham-operated animals were used as controls. The treatment with UK-74,505 or vehicle was administrated (i.v.) 10 min before reperfusion.

Evaluation of changes in vascular permeability

The extravasation of Evans blue dye into the tissue was used as an index of increased vascular permeability, as previously described (Saria & Lundberg, 1983; Souza *et al.*, 2000a). Evans blue (20 mg kg^{-1}) was administered i.v. (1 ml kg^{-1}) *via* a tail vein 2 min prior to reperfusion of the ischemic artery. At 30 min after reperfusion, a segment of the duodenum (approximately 3 cm) was cut open and allowed to dry in a Petri dish for 24 h at 37°C. The dry weight of the tissue was calculated and Evans blue extracted using 1 ml of formamide (24 h at room temperature). The amount of Evans blue in the tissue was obtained by comparing the extracted absorbance with that of a standard Evans blue curve read at 620 nm in an ELISA plate reader. Results are presented as the amount of Evans blue per μg per 100 mg of tissue. The right ventricle was flushed with 10 ml of phosphate-buffered saline (PBS) to wash the intravascular Evans blue in the lungs. The left lung was then excised and used for Evans blue extraction. The right lung was used for the determination of myeloperoxidase as described below.

Myeloperoxidase (MPO) concentrations

The extent of neutrophil accumulation in the intestine and right lung tissue was measured by assaying myeloperoxidase (MPO) activity, as previously described (Kuebler *et al.*, 1996; Souza *et al.*, 2002). Briefly, a portion of duodenum and the flushed right lungs of animals that had undergone I/R injury were removed and snap frozen in liquid nitrogen. Upon thawing and processing, the tissue was assayed for MPO activity by measuring the change in optical density (OD) at 450 nm using tetramethylbenzidine. Results were expressed as the neutrophil infiltration. An index unit denotes the MPO activity present in 10^5 casein-elicited murine peritoneal neutrophils processed in the same way.

Measurement of hemoglobin concentrations

The determination of hemoglobin concentrations in tissue was used as an index of tissue hemorrhage. After washing the intestines to remove excess blood, a sample of approximately 100 mg of duodenum was removed and homogenized in Drabkin's color reagent according to the instructions of the manufacturer (Analisa, Belo Horizonte, Brazil). The suspension was centrifuged for 15 min at 3000 $\times$ *g* and filtered using 0.2 μm filters. The resulting solution was read using an ELISA plate reader at 520 nm and compared against a standard curve of hemoglobin.

Measurement of cytokine/chemokine concentrations in serum, intestine and lungs

The concentration of TNF-α and IL-10 in samples was measured in serum and tissue of animals using commercially available antibodies and according to the procedures supplied by the manufacturer (R&D Systems, Minneapolis). Serum was obtained from coagulated blood (15 min at 37°C, then 30 min at 4°C) and stored at −20°C until further analysis. Serum samples were analyzed at a 1 : 3 dilution in PBS. Duodenum (100 mg) or lung of sham-operated and reperfused animals were homogenized in 1 ml of PBS (0.4 M NaCl and 10 mM de $NaPO_4$) containing antiproteases (0.1 mM phenylmethylsulfonyl fluoride, 0.1 mM benzethonium chloride, 10 mM EDTA and 20 KI aprotinin A) and 0.05% Tween 20. The samples were then centrifuged for 10 min at 3000 $\times$ *g* and the supernatant immediately used for ELISA assays at a 1 : 3 dilution in PBS.

Drugs and reagents

The following drugs were obtained from Sigma (U.S.A.): urethane, Evans blue, hexadecyltrimethylammonium bromide. The PAF receptor antagonist UK-74,505 (modipafant) was a gift of Dr J. Parry (Pfizer, Sandwich, U.K.) (Alabaster *et al.*, 1991). UK-74,505 was dissolved in 0.1 M HCl and further diluted 10-fold in saline just prior to use.

Statistical analysis

Results are shown as means ± s.e.m. Percent inhibition was calculated by subtracting the background values obtained in sham-operated animals. Differences were compared by using analysis of variance (ANOVA) followed by Student–Newman–Keuls *post hoc* analysis. Results with $P<0.05$ were considered significant.

Results

Intestinal I/R injury and lethality in wild-type and PAFR$^{-/-}$ mice

The reperfusion of the ischemic SMA artery induced marked local (intestine) and remote (lungs) tissue injury, as assessed by the increase in vascular permeability, neutrophil influx and intestinal hemorrhage observed in wild-type mice (Figure 1). In contrast, there was a marked and almost complete inhibition of tissue injury in PAFR$^{-/-}$ mice submitted to the same experimental conditions (Figure 1).

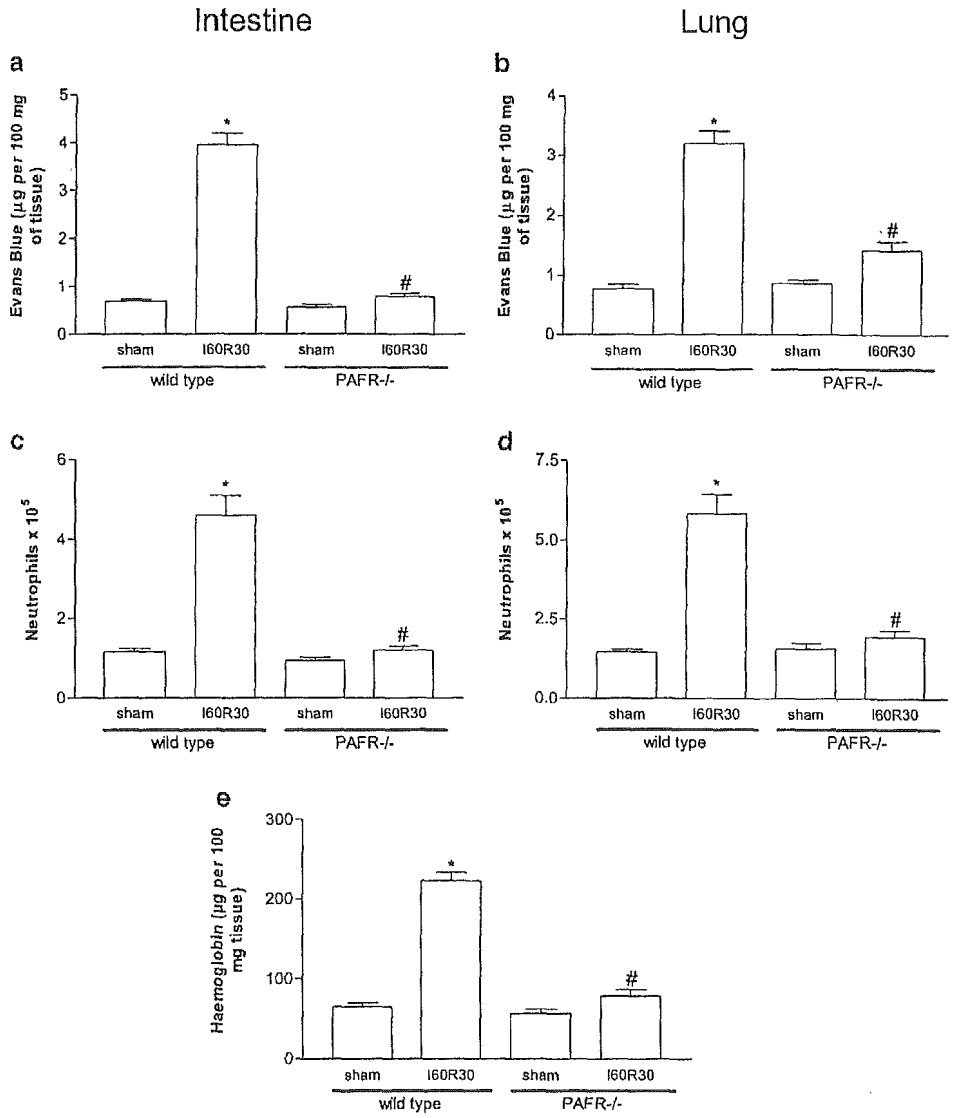

Figure 1 Tissue injury in wild-type (WT) and in PAFR-deficient mice (PAFR$^{-/-}$) submitted to ischemia and reperfusion of the SMA. WT or PAFR$^{-/-}$ were sham-operated or submitted to 60 min of ischemia and 30 min of reperfusion of the SMA. Changes in vascular permeability in the intestine (a) and lungs (b) were evaluated by measuring the extravasation of Evans Blue (µg per 100 mg of tissue). Neutrophil infiltration was determined by measurement of intestinal (c) and pulmonary (d) MPO activity. Hemorrhage in the intestine (e) was evaluated by measuring the concentration of hemoglobin in 100 mg of tissue. Data are shown as the mean ± s.e.m. of five to six mice in each group. *$P<0.01$ when compared with the sham-operated group and $^{\#}P<0.01$ when compared with WT mice submitted to I/R.

In addition to the local and remote inflammatory changes described above, there was a marked increase in the concentrations of TNF-α in the intestine, lungs and serum of wild-type reperfused mice (Figure 2). Again, the increases in the concentration of this cytokine were markedly suppressed in PAFR$^{-/-}$ mice submitted to intestinal I/R (Figure 2). Following reperfusion of the ischemic SMA, the concentrations of the anti-inflammatory cytokine IL-10 were much greater in the intestine and lungs of reperfused PAFR$^{-/-}$ mice than in the tissues of their wild-type controls (Figure 3).

In addition to the observed suppression of tissue and systemic inflammation, there was a significant delay in reperfusion-induced lethality in PAFR$^{-/-}$ (Figure 4). However, delay in lethality was not accompanied by prevention of lethality, as all animals were dead after 90 min of reperfusion (Figure 4).

Effects of the treatment with UK-74,505 on intestinal ischemia and reperfusion injury and lethality

As tissue and systemic inflammation was suppressed and lethality delayed in PAFR$^{-/-}$ mice, it was of interest to examine whether similar effects could be observed after treatment with a PAF receptor antagonist. To this end, UK-74,505, a selective and potent PAFR antagonist, was used at a

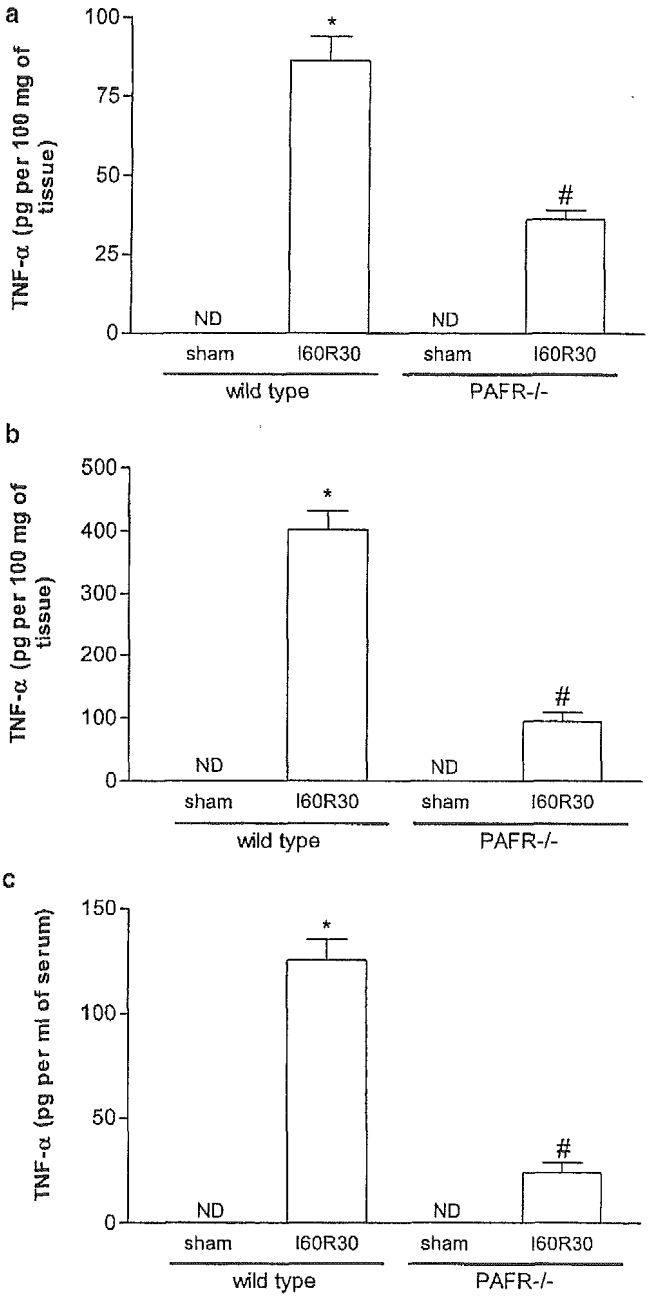

Figure 2 Concentration of TNF-α in the intestine, lungs and serum of WT and in PAFR$^{-/-}$ submitted to ischemia and reperfusion of the SMA. WT or PAFR$^{-/-}$ were sham-operated or submitted to 60 min of ischemia and 30 min of reperfusion of the SMA. The concentrations of TNF-α in intestine (a), lungs (b) and serum (c) were measured by ELISA. Results are shown as picogram of TNF-α per 100 mg of tissue or as picogram TNF-α per milliliter of serum and represent the mean ± s.e.m. of five to six mice in each group. $^{*}P<0.01$ when compared with the sham-operated group and $^{\#}P<0.01$ when compared with WT mice submitted to I/R.

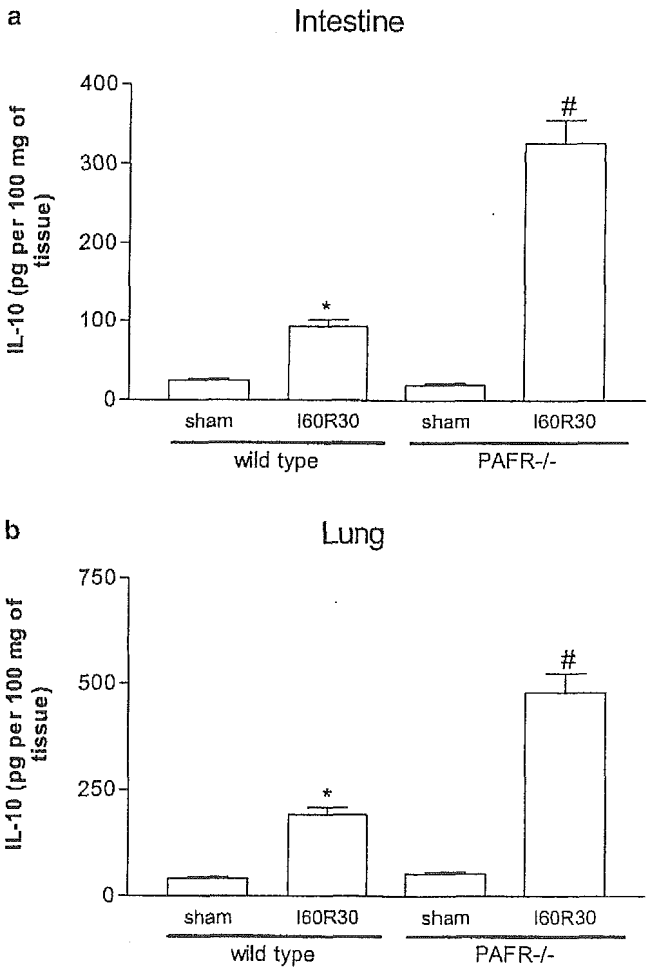

Figure 3 Concentration of IL-10 in the intestine and lungs WT and in PAFR$^{-/-}$ submitted to ischemia and reperfusion of the SMA. WT or PAFR$^{-/-}$ were sham-operated or submitted to 60 min of ischemia and 30 min of reperfusion of the SMA. The concentrations of IL-10 in intestine (a) and lungs (b) were measured by ELISA. Results are shown as picogram of IL-10 per 100 mg of tissue and represent the mean ± s.e.m. of five to six mice in each group. $^{*}P<0.01$ when compared with the sham-operated group and $^{\#}P<0.01$ when compared with wild-type mice submitted to I/R.

dose of 1 mg kg^{-1} that has been previously shown to block PAFR effectively in the mouse or rat (Miotla *et al.*, 1998; Borges *et al.*, 2000; Souza *et al.*, 2000b; Klein *et al.*, 2002). The treatment with UK-74,505 10 min prior to the reperfusion virtually abolished the increases in vascular permeability and influx of neutrophils in the intestine and lungs following intestinal I/R (Table 1). The reperfusion-induced intestinal hemorrhage, as assessed by extravasation of hemoglobin, was abrogated in UK-74,505-treated animals (Table 1).

Interestingly, although the increase in reperfusion-induced tissue concentrations of TNF-α was markedly inhibited by UK-74,505 used at 1 mg kg^{-1}, this dose of the PAFR antagonist had no significant effect on serum concentrations of TNF-α (Figure 5b). Note that the concentrations of TNF-α in the intestine and lungs of UK-74,505-treated mice were equivalent to the concentrations found in reperfused PAFR$^{-/-}$ mice (compare Figure 2 and Table 1). At this dose, UK-74,505 also failed to enhance significantly the increases in IL-10 production in the lungs and intestine following reperfusion of the ischemic SMA (Figure 6). Our previous studies have shown a strong correlation between serum, but not tissue, concentrations of TNF-α and lethality (Souza *et al.*, 2001; 2002). Consistently with these results, treatment of mice with 1 mg kg^{-1} of UK-74,505 had no effect on the lethality that followed reperfusion of the ischemic mesenteric artery (Figure 5a).

The lack of effects of UK-74,505 on reperfusion-associated increase in serum concentrations of TNF-α and lethality was unexpected in the face of the results obtained in PAFR$^{-/-}$ mice. Although the dose of UK-74,505 used has been previously to block PAFR effectively in several *in vivo* systems (Miotla *et al.*, 1998; Borges *et al.*, 2000; Souza *et al.*, 2000b; Klein *et al.*, 2002) and effectively blocked tissue injury in our model, we carried out a series of experiments using a supramaximal dose of the antagonist (10 mg kg^{-1}) reasoning that maximal occupation of the receptor by the antagonist might be necessary to prevent reperfusion-associated lethality. At the higher dose of UK-74,505 used, there was a marked suppression of the reperfusion-induced increase in the serum concentrations of TNF-α (Figure 5b). More importantly, the inhibition of TNF-α was associated with a delay and partial prevention of reperfusion-associated lethality (Figure 5a). Akin to the results observed in PAFR$^{-/-}$ mice, treatment with the higher dose of UK-74,505 markedly enhanced the increases in IL-10 production in the intestine and lung of reperfused mice (Figure 6). To exclude an action of UK-74,505 (10 mg kg^{-1}) outside its effects on the PAFR, PAFR$^{-/-}$ mice were treated with the drug prior to experiments evaluating reperfusion-associated lethality. As seen in Figure 4, the treatment of PAFR$^{-/-}$ with UK-74505 (10 mg kg^{-1}) had no further effect on lethality in addition to that of the PAFR$^{-/-}$ phenotype.

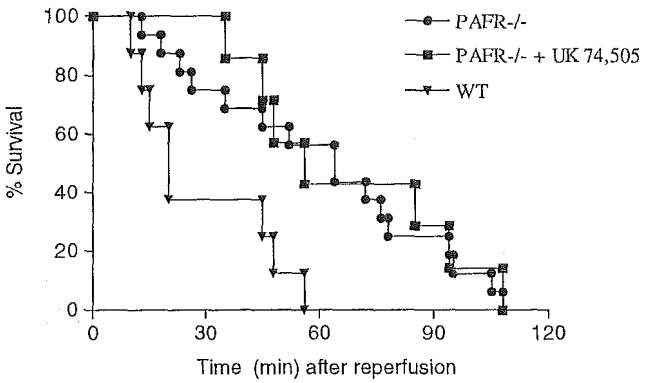

Figure 4 Survival curves of WT and in PAFR$^{-/-}$ submitted to ischemia and reperfusion of the SMA. Mice ($n=10$ in each group) were anesthetized and submitted to ischemia of the SMA for 60 min. Vehicle or UK-74,505 (10 mg kg^{-1}) was administered i.v. 10 min prior to reperfusion. Tissue perfusion was then re-established and survival was monitored. The survival curve of PAFR$^{-/-}$ mice was significantly ($P<0.05$) different from that of WT mice.

Discussion

The restoration of blood flow to an ischemic vascular bed, that is, reperfusion, is a major therapeutic objective after ischemia of an organ or tissue. However, reperfusion may be accompanied by significant local and systemic inflammatory injury, limiting the potential benefits of blood flow restoration. Thus, understanding the pathophysiology of the inflammation that occurs after reperfusion may be useful in the development of novel therapeutic strategies that limit the injury caused by the reperfusion process. Here, the role of PAFR in I/R injury was investigated using mice with a targeted deletion of the PAF receptor gene (Ishii *et al.*, 1998) and the PAFR antagonist UK-74,505 (Alabaster *et al.*, 1991).

Table 1 Effects of the postischemic treatment with the PAF receptor antagonist, UK-74,505 (1 mg kg^{-1}) on the tissue injury in the intestine and lungs of mice submitted to ischemia and reperfusion of the superior mesenteric artery (SMA)

	Intestine			*Lung*		
	Sham	*Vehicle*	*UK*	*Sham*	*Vehicle*	*UK*
Evans Blue	0.7±0.1	4.0±0.2	1.3±0.1	0.8±0.1	3.2±0.2	1.1±0.1
MPO	1.2±0.1	4.6±0.5	1.6±0.1	1.5±0.1	5.8±0.6	2.1±0.2
Hemoglobin	64.6±5.3	223±10.5	79.6±6.7	—	—	—
TNF	ND	86.2±8.0	38.7±4.0	ND	401.3±31	162.5±18.3

Changes in vascular permeability were evaluated by measuring the extravasation of Evans Blue (μg per 100 mg of tissue), neutrophil infiltration was determined by measurement of tissue myeloperoxidase activity, hemorrhage by measuring the concentration of hemoglobin in 100 mg of tissue and concentrations of TNF-α in intestine and lungs by ELISA. UK-74,505 (1 mg kg^{-1}) was given i.v. 5 min prior to reperfusion and control animals received vehicle. Results are shown as picogram of TNF-α per 100 mg of tissue and represent the mean±s.e.m. of six mice in each group. $^{*}P<0.01$ when comparing to the sham-operated group and $^{\#}P<0.01$ when comparing to vehicle-treated mice submitted to I/R.

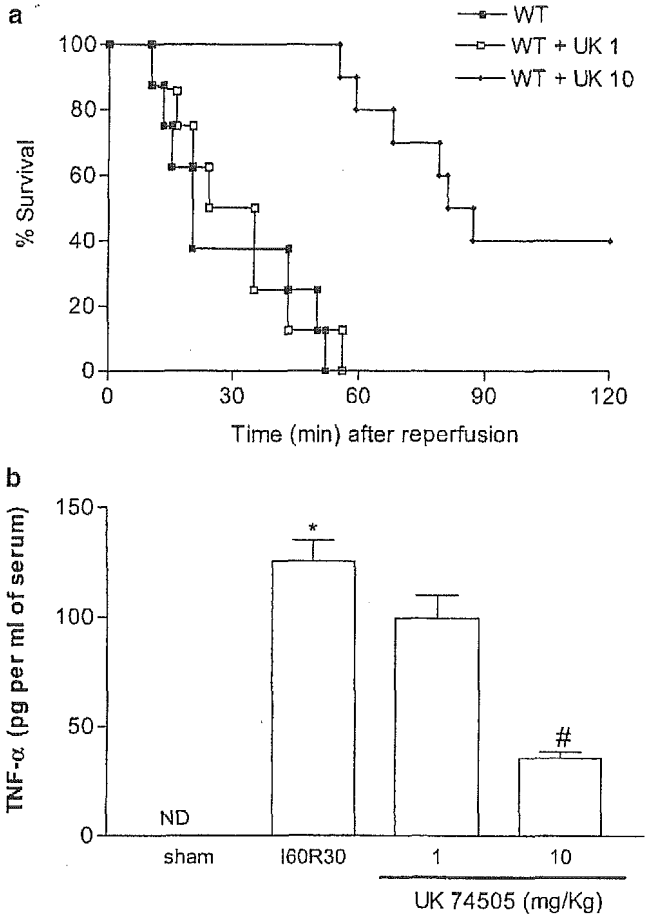

Figure 5 Effects of postischemic treatment with the PAF receptor antagonist UK-74,505 on the (a), survival and (b) serum concentration of TNF-α in mice submitted to ischemia and reperfusion of the SMA. In (a) mice treated with UK-74,505 (1 or 10 mg kg^{-1}) or vehicle ($n=10$ in each group) were anesthetized and submitted to ischemia of the SMA for 60 min. Tissue perfusion was then re-established and survival was monitored. The survival curve of UK-74,505-treated mice (10 mg kg^{-1}) was significantly ($P<0.05$) different from that of vehicle-treated mice. In (b), mice were sham-operated or submitted to 60 min of ischemia of the SMA and reperfusion was allowed for 30 min. Concentrations of TNF-α serum were measured by ELISA. Results are shown as picogram of TNF-α per milliliter of serum and represent the mean ± s.e.m. of six mice in each group. $^{*}P<0.01$ when compared with the sham-operated group and $^{\#}P<0.01$ when compared with vehicle-treated mice submitted to I/R.

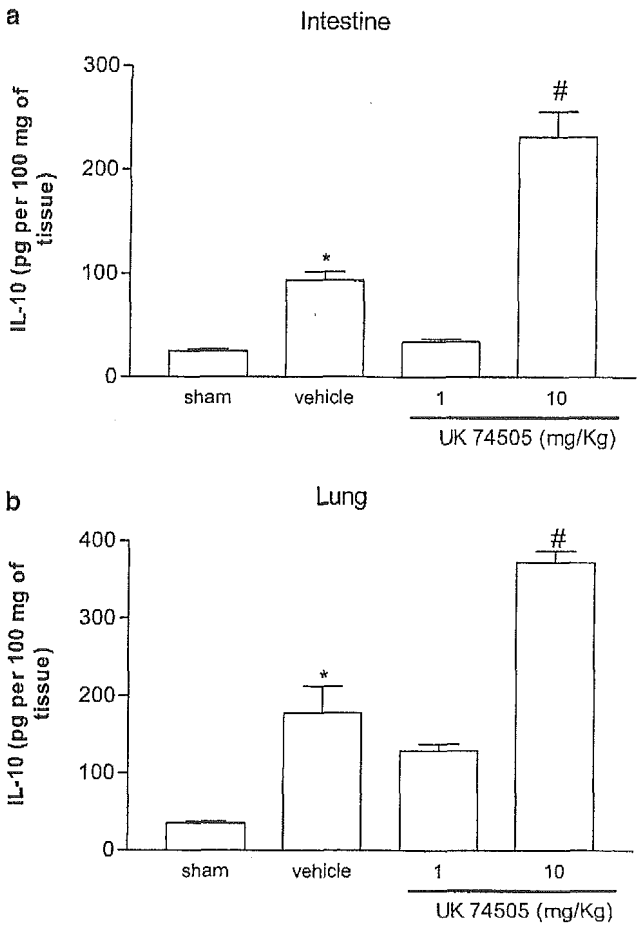

Figure 6 Effects of postischemic treatment with the PAF receptor antagonist UK-74,505 on the concentrations of IL-10 (a) intestine and (b) lungs in mice submitted to ischemia and reperfusion of the SMA. Mice were sham-operated or submitted to 60 min of ischemia of the SMA and reperfusion was allowed for 30 min. UK-74,505 (1 or 10 mg kg^{-1}) was given i.v. 5 min prior to reperfusion. Control animal received vehicle. Concentrations of IL-10 in the intestine (a) and lungs (b) were measured by ELISA. Results are shown as pg of IL-10 per 100 mg of tissue and represent the mean ± s.e.m. of six mice in each group. $^{*}P<0.01$ when comparing to the sham-operated group and $^{\#}P<0.01$ when compared with vehicle-treated mice submitted to I/R.

PAFR$^{-/-}$ mice have been shown to have a normal response to LPS administration, but were extremely resistant to antigen-induced systemic anaphylaxis (Ishii *et al.*, 1998) and to hydrochloric acid aspiration-induced lung injury (Nagase *et al.*, 1999). In addition to playing a role during inflammatory tissue injury caused by different stimuli, we have recently shown that PAFR$^{-/-}$ mice were more susceptible to *Klebsiella pneumoniae* pulmonary infection (Soares *et al.*, 2002) and to *Trypanosoma cruzi* infection (Talvani *et al.*, 2003). Of interest, the protective role of PAFR during infection appeared to be largely related to the relevance of this receptor in mediating phagocytosis of the bacteria or the parasites (Soares *et al.*, 2002; Talvani *et al.*, 2003). In the present study, we show that the inflammatory injury that follows intestinal I/R is markedly inhibited in PAFR$^{-/-}$ mice when compared to their wild-type controls. Thus, there was no increase in vascular permeability, neutrophil accumulation and hemorrhage in the intestine and lung of reperfused PAFR$^{-/-}$ mice. In PAFR$^{-/-}$ mice, the reperfusion-associated increases in serum concentration of TNF-α was significantly suppressed and this was associated with an increase in the concentrations of IL-10. Additionally, there was a significant delay in reperfusion-associated lethality in PAFR$^{-/-}$ mice. These results strongly corroborate the role of PAFR during I/R tissue injury and, to the best of our knowledge, are the first demonstration that the PAFR plays a relevant role for reperfusion-associated lethality.

Several studies, including one of our own, have shown that blockade of PAFR with receptor antagonists blocks the inflammatory injuries that occur following I/R of several vascular beds (Canale *et al.*, 1994; Carter *et al.*, 1996; Riera *et al.*, 1997; Qayumi *et al.*, 1998; Morgan *et al.*, 1999; Kecskemeti & Balogh, 2000; Kim *et al.*, 2000; Souza *et al.*, 2000b; Sun *et al.*, 2001; 2002). It was, thus, of interest to

examine whether pharmacological antagonism of PAFR would prevent tissue injury and lethality, as observed in PAFR$^{-/-}$ mice. To this end, we used the long-acting and selective PAF receptor antagonist, UK-74,505 (Alabaster *et al.*, 1991). In rats, UK-74,505 markedly blocked the severe injuries that followed prolonged I/R of the SMA (Souza *et al.*, 2000b). Maximal inhibition occurred at the dose of 1 mg kg^{-1}. Similar to our previous studies in rats, postischemic treatment with UK-74,505 suppressed the increase in vascular permeability, neutrophil influx and hemorrhage induced by reperfusion of the ischemic SMA. In addition to inhibiting the above-mentioned parameters, UK-74,505 effectively suppressed reperfusion-induced increases in the concentration of TNF-α in tissues. Overall, these results are in agreement with other studies demonstrating a role for PAFR during I/R injury (Canale *et al.*, 1994; Carter *et al.*, 1996; Riera *et al.*, 1997; Qayumi *et al.*, 1998; Morgan *et al.*, 1999; Kecskemeti & Balogh, 2000; Kim *et al.*, 2000; Sun *et al.*, 2001; 2002). In contrast, at the lower dose used, UK-74,505 failed to affect reperfusion-induced increase in serum concentrations of TNF-α and lethality. As neutrophil influx is essential for tissue production of TNF-α (Souza *et al.*, 2000b; 2001), the inhibitory effects of UK-74,505 on tissue TNF-α concentrations may be secondary to its ability to suppress neutrophil influx. However, the inability of UK-74,505 to affect serum TNF-α concentrations and lethality was surprising, as we used a previously shown effective dose of the drug (in the present experiments, tissue injury was abolished) and PAFR$^{-/-}$ mice had diminished amounts of serum TNF-α and delayed lethality.

Although tissue injury was abolished by the lower dose of UK-74,505, it was possible that the mechanisms underlying serum TNF-α production and ensuing lethality relied on PAFR not totally inhibited by the lower dose of the drug. In support of this possibility, intracellular PAFR that are relevant for proinflammatory cytokine production have been recently demonstrated on neutrophils (Marrache *et al.*, 2002). Thus, it is feasible that higher doses (and hence intracellular concentrations) of UK-74,505 are necessary to block this intracellular receptor. Alternatively and akin to previous studies demonstrating the effects of selectin inhibition during I/R injury, it is possible that a virtually complete blockade of PAFR is necessary if inhibition of systemic TNF-α and lethality is to occur (Kubes *et al.*, 1995). Regardless of the underlying explanation for our results, they clearly showed that the use of a higher dose (10 mg kg^{-1}) of UK-74,505 was associated with effective inhibition of serum TNF-α release and delay and prevention of lethality. Interestingly and similar to results seen in PAFR$^{-/-}$ mice, the higher dose of UK-74,505 enhanced the reperfusion-associated increase in tissue concentrations of IL-10. Overall, these results demonstrate that a high dose of PAFR antagonists is needed if we are to delay and/or suppress lethality, in addition to suppressing tissue injury. Whether the need for the use of a high dose of UK-74,505 reflects inhibition of an intracellular PAFR is not known at present, but clearly deserves further investigation. Another relevant observation was that the high dose of UK-74,505 was more effective in preventing lethality than the genetic strategy, suggesting that compensatory mechanisms may be operative in PAFR$^{-/-}$ mice. One alternative explanation to our results was the possibility that UK-74,505 was having an effect distinct from its action on the PAFR. To address this possibility, we administered UK-74,505 (10 mg kg^{-1}) to PAFR$^{-/-}$ mice and evaluated reperfusion-induced lethality. There was no prevention of lethality in addition to that observed in PAFR$^{-/-}$ mice, suggesting that the effects of high-dose UK-74,505 were still related to the ability of the drug to block the PAFR and not because of nonspecific effects.

Finally, the inhibition of reperfusion-associated increases in serum TNF-α concentration and lethality was associated with an enhanced production of IL-10. Other studies have shown that the endogenous IL-10 produced in response to I/R injury may protect the tissue from excess injury (e.g. Frangogiannis *et al.*, 2000; Zingarelli *et al.*, 2001). Whether the IL-10 produced in response to PAFR blockade or in PAFR$^{-/-}$ mice is relevant for the suppressive effects observed is not known. Moreover, the observation that the enhancement of IL-10 production is only observed when a high dose of UK-74,505 or PAFR$^{-/-}$ mice are used is intriguing and may suggest that the activation of intracellular PAFR may play a role in controlling not only proinflammatory, but also anti-inflammatory, cytokines (Marrache *et al.*, 2002). This possibility needs further investigation.

In conclusion, our studies using genetically modified animals and receptor antagonists firmly establish a role of PAFR activation for the local, remote and systemic inflammatory injury and lethality, which follows reperfusion of the ischemic SMA in mice. Whereas tissue injury was inhibited by a lower dose of the PAFR antagonist UK-74,505, lethality was only suppressed when a higher dose of the compound was used. These results suggest that high doses of PAFR antagonists need to be used if the real efficacy of these compounds is to be tested clinically.

We thank the Conselho Nacional de Desenvolvimento Científico e Tecnológico (CNPq) and Fundação de Amparo a Pesquisas do Estado de Minas Gerais (FAPEMIG) for financial support.

References

ALABASTER, V.A., KEIR, R.F., PARRY, M.J. & DE SOUZA, R.N. (1991). UK-74,505, a novel and selective PAF antagonist, exhibits potent and long lasting activity *in vivo*. *Agents Actions Suppl.*, **34**, 221–227.

BORGES, C.M., SILVEIRA, M.R., APARECIDA, M., BEKER, C.L., FREIRE-MAIA, L. & TEIXEIRA, M.M. (2000). Scorpion venom-induced neutrophilia is inhibited by a PAF receptor antagonist in the rat. *J. Leukoc. Biol.*, **67**, 515–519.

CANALE, P., SQUADRITO, F., ALTAVILLA, D., IOCULANO, M., ZINGARELLI, B., CAMPO, G.M., URNA, G., SARDELLA, A., SQUADRITO, G. & CAPUTI, A.P. (1994). TCV-309, a novel platelet activating factor antagonist, inhibits leukocyte accumulation and protects against splanchnic artery occlusion shock. *Agents Actions*, **42**, 128–134.

CARDEN, D.L. & GRANGER, D.N. (2000). Pathophysiology of ischaemia–reperfusion injury. *J. Pathol.*, **90**, 255–266.

CARTER, M.B., WILSON, M.A., WEAD, W.B. & GARRISON, R.N. (1996). Platelet-activating factor mediates pulmonary macromolecular leak following intestinal ischemia–reperfusion. *J. Surg. Res.*, **60**, 403–408.

FRANGOGIANNIS, N.G., MENDOZA, L.H., LINDSEY, M.L., BALLANTYNE, C.M., MICHAEL, L.H., SMITH, C.W. & ENTMAN, M.L.

(2000). IL-10 is induced in the reperfused myocardium and may modulate the reaction to injury. *J. Immunol.*, **165**, 2798–2808.

GRANGER, D.N. (1999). Ischemia–reperfusion: mechanisms of microvascular dysfunction and the influence of risk factors for cardiovascular disease. *Microcirculation*, **6**, 167–178.

ISHII, S., KUWAKI, T., NAGASE, T., MAKI, K., TASHIRO, F., SUNAGA, S., CAO, W.H., KUME, K., FUKUCHI, Y., IKUTA, K., MIYAZAKI, J., KUMADA, M. & SHIMIZU, T. (1998). Impaired anaphylactic responses with intact sensitivity to endotoxin in mice lacking a platelet-activating factor receptor. *J. Exp. Med.*, **187**, 1779–1788.

KECSKEMETI, V. & BALOGH, I. (2000). The role of platelet-activating factor (PAF) antagonists and nitric oxide in cardiac actions of PAF. Electrophysiological and morphological study. *J. Physiol. Pharmacol.*, **51**, 723–735.

KIM, J.D., BAKER, C.J., ROBERTS, R.F., DARBINIAN, S.H., MARCUS, K.A., QUARDT, S.M., STARNES, V.A. & BARR, M.L. (2000). Platelet activating factor acetylhydrolase decreases lung reperfusion injury. *Ann. Thorac. Surg.*, **70**, 423–428.

KLEIN, A., PINHO, V., ALESSANDRINI, A.L., SHIMIZU, T., ISHII, S. & TEIXEIRA, M.M. (2002). Platelet-activating factor drives eotaxin production in an allergic pleurisy in mice. *Br. J. Pharmacol.*, **135**, 1213–1218.

KUBES, P., IBBOTSON, G., RUSSELL, J., WALLACE, J.L. & GRANGER, D.N. (1990a). Role of platelet-activating factor in ischemia/reperfusion-induced leukocyte adherence. *Am. J. Physiol.*, **259**, G300–G305.

KUBES, P., JUTILA, M. & PAYNE, D. (1995). Therapeutic potential of inhibiting leukocyte rolling in ischemia/reperfusion. *J. Clin. Invest.*, **95**, 2510–2519.

KUBES, P., SUZUKI, M. & GRANGER, D.N. (1990b). Platelet-activating factor-induced microvascular dysfunction: role of adherent leukocytes. *Am. J. Physiol.*, **258**, G158–G163.

KUEBLER, W.M., ABELS, C., SCHUERER, L. & GOETZ, A.E. (1996). Measurement of neutrophil content in brain and lung tissue by a modified myeloperoxidase assay. *Int. J. Microcirc. Clin. Exp.*, **16**, 89–97.

LEFER, A.M. & LEFER, D.J. (1996). The role of nitric oxide and cell adhesion molecules on the microcirculation in ischaemia–reperfusion. *Cardiovasc. Res.*, **32**, 743–751.

MARRACHE, A.M., GOBEIL JR, F., BERNIER, S.G., STANKOVA, J., ROLA-PLESZCZYNSKI, M., CHOUFANI, S., BKAILY, G., BOURDEAU, A., SIROIS, M.G., VAZQUEZ-TELLO, A., FAN, L., JOYAL, J.S., FILEP, J.G., VARMA, D.R., RIBEIRO-DA-SILVA, A. & CHEMTOB, S. (2002). Proinflammatory gene induction by platelet-activating factor mediated *via* its cognate nuclear receptor. *J. Immunol.*, **169**, 6474–6481.

MIOTLA, J.M., JEFFERY, P.K. & HELLEWELL, P.G. (1998). Platelet-activating factor plays a pivotal role in the induction of experimental lung injury. *Am. J. Respir. Cell Mol. Biol.*, **18**, 197–204.

MONTRUCCHIO, G., ALLOATTI, G. & CAMUSSI, G. (2000). Role of platelet-activating factor in cardiovascular pathophysiology. *Physiol. Rev.*, **80**, 1669–1699.

MORGAN, E.N., BOYLE JR, E.M., YUN, W., KOVACICH, J.C., CANTY JR, T.G., CHI, E., POHLMAN, T.H. & VERRIER, E.D. (1999). Platelet-activating factor acetylhydrolase prevents myocardial ischemia–reperfusion injury. *Circulation*, **100**, II365–II368.

NAGASE, T., ISHII, S., KUME, K., UOZUMI, N., IZUMI, T., OUCHI, Y. & SHIMIZU, T. (1999). Platelet-activating factor mediates acid-induced lung injury in genetically engineered mice. *J. Clin. Invest.*, **104**, 1071–1076.

QAYUMI, A.K., ENGLISH, J.C., GODIN, D.V., ANSLEY, D.M., LOUCKS, E.B., LEE, J.U. & KIM, C.W. (1998). The role of platelet-activating factor in regional myocardial ischemia–reperfusion injury. *Ann. Thorac. Surg.*, **65**, 1690–1697.

RIERA, M., TORRAS, J., HERRERO, I., VALLES, J., PAUBERT-BRAQUET, M., CRUZADO, J.M., ALSINA, J. & GRINYO, J.M. (1997). Neutrophils accentuate renal cold ischemia–reperfusion injury. Dose-dependent protective effect of a platelet-activating factor receptor antagonist. *J. Pharmacol. Exp. Ther.*, **280**, 786–794.

SARIA, A. & LUNDBERG, J.M. (1983). Evans blue fluorescence: quantitative and morphological evaluation of vascular permeability in animal tissues. *J. Neurosci. Methods*, **8**, 41–49.

SOARES, A.C., PINHO, V.S., SOUZA, D.G., SHIMIZU, T., ISHII, S., NICOLI, J.R. & TEIXEIRA, M.M. (2002). Role of the platelet-activating factor (PAF) receptor during pulmonary infection with Gram negative bacteria. *Br. J. Pharmacol.*, **137**, 621–628.

SOUZA, D.G., COUTINHO, S.F., SILVEIRA, M.R., CARA, D.C. & TEIXEIRA, M.M. (2000a). Effects of a BLT receptor antagonist on local and remote reperfusion injuries after transient ischemia of the superior mesenteric artery in rats. *Eur. J. Pharmacol.*, **403**, 121–128.

SOUZA, D.G., CARA, D.C., CASSALI, G.D., COUTINHO, S.F., SILVEIRA, M.R., ANDRADE, S.P., POOLE, S.P. & TEIXEIRA, M.M. (2000b). Effects of the PAF receptor antagonist UK74505 on local and remote reperfusion injuries following ischaemia of the superior mesenteric artery in the rat. *Br. J. Pharmacol.*, **131**, 1800–1808.

SOUZA, D.G., CASSALI, G.D., POOLE, S. & TEIXEIRA, M.M. (2001). Effects of inhibition of PDE4 and TNF-alpha on local and remote injuries following ischaemia and reperfusion injury. *Br. J. Pharmacol.*, **134**, 985–994.

SOUZA, D.G., SOARES, A.C., PINHO, V., TORLONI, H., REIS, L.F., TEIXEIRA, M.M. & DIAS, A.A. (2002). Increased mortality and inflammation in tumor necrosis factor-stimulated gene-14 transgenic mice after ischemia and reperfusion injury. *Am. J. Pathol.*, **160**, 1755–1765.

SUN, Z., WANG, X., LASSON, A., BOJESSON, A., ANNBORN, M. & ANDERSSON, R. (2001). Effects of inhibition of PAF, ICAM-1 and PECAM-1 on gut barrier failure caused by intestinal ischemia and reperfusion. *Scand. J. Gastroenterol.*, **36**, 55–65.

SUN, Z., OLANDERS, K., LASSON, A., DIB, M., ANNBORN, M., ANDERSSON, K., WANG, X. & ANDERSSON, R. (2002). Effective treatment of gut barrier dysfunction using an antioxidant, a PAF inhibitor, and monoclonal antibodies against the adhesion molecule PECAM-1. *J. Surg. Res.*, **105**, 220–233.

TALVANI, A., BARCELOS, L., SANTANA, G., ISHII, S., SHIMIZU, T., ROMANHA, A.J., SILVA, J.S., SOARES, M.B.P. & TEIXEIRA, M.M. (2003). Experimental *Trypanosoma cruzi* infection in PAFR-deficient mice. *Microb Inf.* (in press).

ZINGARELLI, B., YANG, Z., HAKE, P.W., DENENBERG, A. & WONG, H.R. (2001). Absence of endogenous interleukin 10 enhances early stress response during post-ischaemic injury in mice intestine. *Gut*, **48**, 610–622.

(Received January 6, 2003
Revised March 13, 2003
Accepted March 25, 2003)

Available online at www.sciencedirect.com
SCIENCE DIRECT®
Microbes and Infection 5 (2003) 789–796
Microbes and Infection
www.elsevier.com/locate/micinf

Original article

Experimental *Trypanosoma cruzi* infection in platelet-activating factor receptor-deficient mice

André Talvani [a], Gilcinea Santana [a], Lucíola S. Barcelos [a], Satoshi Ishii [b,c], Takao Shimizu [b,c], Álvaro J. Romanha [d], João S. Silva [e], Milena B.P. Soares [f], Mauro M. Teixeira [a,d,*]

[a] *Departamento de Bioquímica e Imunologia, Instituto de Ciências Biológicas, Universidade Federal de Minas Gerais, Avenida Antônio Carlos, 6627 Pampulha, 31270-901 Belo Horizonte, Minas Gerais, Brazil*
[b] *Department of Biochemistry and Molecular Biology, Faculty of Medicine, The University of Tokyo, Japan*
[c] *CREST of Japan Science and Technology Corporation, Tokyo, Japan*
[d] *Centro de Pesquisas René Rachou, FIOCRUZ, Belo Horizonte,Brazil*
[e] *Faculdade de Medicina de Ribeirão Preto, Universidade de São Paulo, Ribeirão Preto, São Paulo, Brazil*
[f] *Centro de Pesquisa Gonçalo Moniz, FIOCRUZ, Salvador, Brazil*

Received 19 December 2002; accepted 31 March 2003

Abstract

The generation of an inflammatory response driven by *Trypanosoma cruzi* or its subproducts appears to be essential for tissue injury and disease pathogenesis. However, this inflammatory response is also relevant in the control of *T. cruzi* replication. The lipid mediator platelet-activating factor (PAF) has been implicated in a number of pathological conditions characterized by tissue inflammation. In the present study, we aimed at evaluating the role of PAF during *T. cruzi* infection by using mice that were genetically deficient in the PAF receptor. We observed that infected hearts of $PAFR^{-/-}$ mice had an increased number of parasite nests, associated with a more intense inflammatory infiltrate. This was associated with greater parasitemia and lethality. When wild-type and $PAFR^{-/-}$ mice were compared, there were no marked changes in the kinetics of the expression of MCP-1, RANTES, IFN-γ and TNF-α in heart tissue of infected animals. Moreover, serum concentrations of TNF-α, nitrate and parasite-specific IgM were similar in both groups of mice. In vitro, macrophages from $PAFR^{-/-}$ animals did not phagocytose trypomastigote forms when activated with PAF, leukotriene B_4 or MCP-1 and produced less nitric oxide when infected and activated with IFN-γ. These results are consistent with the hypothesis that endogenous synthesis of PAF and activation of PAF receptors control *T. cruzi* replication in mice in great part via facilitation of the uptake of the parasite and consequent activation of macrophages.

Keywords: Platelet-activating factor; Protozoan infection; Inflammation; Chemokines; TNF-α; Knockout

1. Introduction

Chagas' disease, a common cause of congestive heart failure and sudden death in South and Central America, is caused by a hemoflagellate parasite, *Trypanosoma cruzi*, which is widely distributed in this geographic area [1,2]. The generation of an inflammatory response driven by *T. cruzi* or its subproducts appears to be essential for tissue injury and disease pathogenesis [3,4]. In addition to parasite-driven inflammation, an autoimmune component may also play a role in the tissue damage during the chronic stages of the disease, especially in cardiac tissues [5–7]. The inflammation observed in infected tissues is characterized by the infiltration of $CD4^+$ and $CD8^+$ T cells and macrophages, which appear to secrete a range of cytokines, chemokines, oxygen reactive products and other inflammatory mediators, such as platelet-activating factor (PAF) and leukotriene B_4 (LTB_4) [3,8–13]. Although inflammation determines tissue damage, the cellular influx and mediators formed in response to parasite invasion appear to be relevant in the control of *T. cruzi* replication. The question of whether a similar set of mediators is responsible for tissue damage and defense against the parasite clearly deserves investigation.

The lipid mediator PAF (1-0-alkyl-2-acetyl-*sn*-glyceryl-3-phosphorocholine), is produced by a diverse number of inflammatory cells, including macrophages, neutrophils, ba-

* Corresponding author.
Tel.: +55-31-3499-2651; fax: +55-31-3441-5963.
E-mail address: mmtex@icb.ufmg.br (M.M. Teixeira).

DOI: 10.1016/S1286-4579(03)00146-1

sophils, eosinophils, platelets and endothelial cells [14,15]. PAF has been implicated in a number of pathological conditions, including endotoxic shock, thrombosis, allergic reactions and a variety of other inflammatory conditions [14–16]. Studies on immunity to *T. cruzi* infection have focused on the relationship between cytokines/chemokines and production of nitric oxide (NO) and oxygen intermediates [3,4,8,17,18]. The involvement of other mediators, such as those derived from membrane metabolism, in immunity to *T. cruzi* has been largely ignored. More recently, our group demonstrated that PAF and another lipid mediator, LTB_4, were able to induce NO and tumor necrosis factor-α (TNF-α) synthesis in cultured *T. cruzi*-infected peritoneal macrophages and kill the parasite in a NO-dependent manner [12,19]. In vivo, blockade of PAF or LTB_4 receptors was accompanied by higher parasitemia and lower survival of infected animals [12,19].

In the present study, we aimed at evaluating the protective role of PAF during *T. cruzi* infection by using mice that were genetically deficient in the PAF receptor [20]. Moreover, we evaluated several aspects of the inflammatory response and parasitological indices during *T. cruzi* infection in an attempt to identify mechanisms involved in the protective effects of PAF in our model. We observed that infected hearts of $PAFR^{-/-}$ mice had an increased number of parasite nests, associated with a more intense inflammatory infiltrate. This was associated with greater parasitemia and lethality. In vitro, macrophages from $PAFR^{-/-}$ animals did not phagocytose trypomastigote forms when activated with PAF, LTB_4 or MCP-1 and produced less NO when infected and activated with IFN-γ. Together with our previous studies [12,19], our results are consistent with the hypothesis that endogenous synthesis of PAF and activation of PAF receptors control *T. cruzi* replication in mice in great part via facilitation of the phagocytosis of the parasite and consequent activation of macrophages.

2. Materials and methods

2.1. Experimental animals

Female C57BL/6 wild-type and PAF receptor-deficient mice [20] were bred at Centro de Pesquisas Gonçalo Muniz, FIOCRUZ (Salvador, Brazil) and maintained under standard conditions in the animal house of our institution. Animals were used when 8–10 weeks old. All procedures had prior approval from the local animal ethics committee.

2.2. Parasites and experimental infection

The Y strain of *T. cruzi* was used in all experiments. Trypomastigote forms were cultured and purified from the monkey kidney fibroblast cell line LLC-MK2 for experiments in vitro. C57BL/6 mice were infected intraperitoneally with 5×10^3 blood trypomastigote forms, and parasitemia was evaluated daily by counting the number of parasites in 5 μl of blood from a tail vein, as previously described [21].

2.3. Macrophage culture

Inflammatory macrophages were harvested from the peritoneal cavity of mice 3 d after the injection of 1.5 ml of 3% (w/v) sodium thioglycolate (Sigma). Cells (10^6/ml) were plated onto chamber slides in 24-well tissue culture plates and incubated for 2–4 h at 37 °C. The non-adherent cells were removed by exhaustive washing with Hank's medium. Adherent cells were then infected at a parasite-to-cell ratio of 1:1 for 120 min. After incubation with *T. cruzi*, extracellular parasites were removed by six washes with RPMI-1640 and infected macrophages were incubated at 37 °C in 5% CO_2 in the presence or absence of 50 U/ml of recombinant murine IFN-γ (Life Technologies, Bethesda, Md.) for 48 h. Supernatants from these infected cultured peritoneal macrophages were collected to measure NO_2 + NO_3 (NO_x) levels, as described below.

In parallel experiments, the uptake of trypomastigote forms by macrophages was evaluated in vitro [17]. Macrophages (10^6/ml) derived from the peritoneal cavity of wild-type or $PAFR^{-/-}$ mice were plated onto glass slides that fitted 48-well plates. After washing to remove non-adherent cells, macrophages were treated with PAF (10^{-7} M), LTB_4 (10^{-6} M) or MCP-1 (10^{-7} M) for 10 min. Parasites were added in a 2:1 parasite:cell ratio, and 2 h later the extracellular trypomastigote forms were removed by washing with RPMI-1640. The macrophages were fixed with methanol and stained with Giemsa solution (1:20) in order to determine the number of intracellular amastigotes. At least 200 macrophages were analyzed on each slide, and all experiments were carried out in triplicate.

2.4. NO_x measurement in vivo and in vitro

Nitrite levels in supernatants of infected macrophage cultures were determined using the Griess reaction, as an index of the NO produced [22]. To determine the levels of NO_x in vivo, blood was collected on different days before sacrifice of infected wild-type and transgenic animals. Serum was obtained from these samples, and NO_x was measured using the Griess reaction [22] after treatment of samples with nitrate reductase [23].

2.5. TNF-α, IFN-γ, RANTES and MCP-1 measurement

Left and right ventricles from wild-type and $PAFR^{-/-}$ mouse hearts were homogenized in phosphate-buffered saline (PBS) pH 7.4, centrifuged at 1000 rpm at 4 °C and supernatants were stored at –70 °C. The concentrations of TNF-α, IFN-γ, MCP-1 and RANTES in cardiac extracts were evaluated by ELISA using commercially available antibodies and according to the protocol provided by the supplier (duo-set R&D Systems).

2.6. IgM ELISA

Flat-bottom 96-well microtiter plates (Nunc) were coated with 100 μl/well of the *T. cruzi* epimastigote antigen

(10 µl/ml) at 4 °C overnight and then washed with 1× PBS (pH 7.4) containing 0.05% Tween-20 (wash buffer). Non-specific binding sites were blocked 2 h with 200 ml/well of 1% BSA in PBS. Plates were rinsed with wash buffer and 1:100 diluted serum samples were added (100 µl/well), followed by incubation for 1 h at room temperature. Plates were then washed and 100 µl/well of the anti-IgM biotinylated detection antibodies 1:20,000 diluted in wash buffer were added for 1 h at room temperature. After that, plates were newly washed, 1:4000 wash buffer diluted streptavidin-horseadish peroxidase was added (100 µl/well), and the plates were incubated for 30 min at room temperature. Plates were then washed, 100 µl/well of the 0.04% chromogen substrate OPD (*o*-phenylendiamide, Sigma) diluted in citrate buffer (pH 5.0) containing 0.02% 30 v/v H_2O_2 was added, and the plates were incubated in the dark for 30 min at room temperature. The reaction was terminated with 50 µl/well of 1M H_2SO_4 solution. Plates were read at 492 nm in a spectrophotometer (E max–Molecular Devices). All samples were assayed in duplicate.

2.7. Histology

Hearts were removed at necropsy, and sections were immediately fixed in 10% phosphate-buffered formalin. After fixation, sections were prepared by standard methods for paraffin-embedded blocks, and cut sections were stained with hematoxylin and eosin. Cardiac parasitism and inflammation of ventricles were estimated in three different 7-µm-depth sections in each heart, and five different animals were analyzed in each group. Amastigote nests and inflammation were assessed with a Zeiss (Öberkohen, Germany) integrating eyepiece, with 100 hits at a final magnification of 400×. A total of 3000 hits was evaluated in each section of cardiac tissue. The infection index represents the number of hits covered by amastigote nests, and the inflammatory index represents the number of hits in which inflammatory cells were present.

2.8. Statistical analysis

All results are presented as the mean ± S.E.M. Normalized data were analyzed by one-way ANOVA and differences between groups were assessed using the Student–Newman–Keuls post-test. A value of $P < 0.05$ was considered to be significant. All analyses were made using the INSTAT program (Graph PAD Software, Inc. San Diego, California).

3. Results

3.1. Infection indices in T. cruzi-infected PAFR$^{-/-}$ mice

We have previously shown that blockade of PAFR with the PAFR antagonist WEB-2170 [2] or UK-74,505 (our own unpublished data) was associated with increased parasitemia following infection with 5×10^3 *T. cruzi* trypomastigotes. Here, parasitemia in PAFR$^{-/-}$ mice was approximately twice that of C57BL/6 wild-type mice at the peak of parasitemia (Fig. 1A). More importantly, the survival of infected PAFR$^{-/-}$ mice was lower than that of infected wild-type mice (Fig. 1B). Indeed, 15 d after infection, none of the PAFR$^{-/-}$ mice, but around 70% of wild-type animals were alive (Fig. 1B).

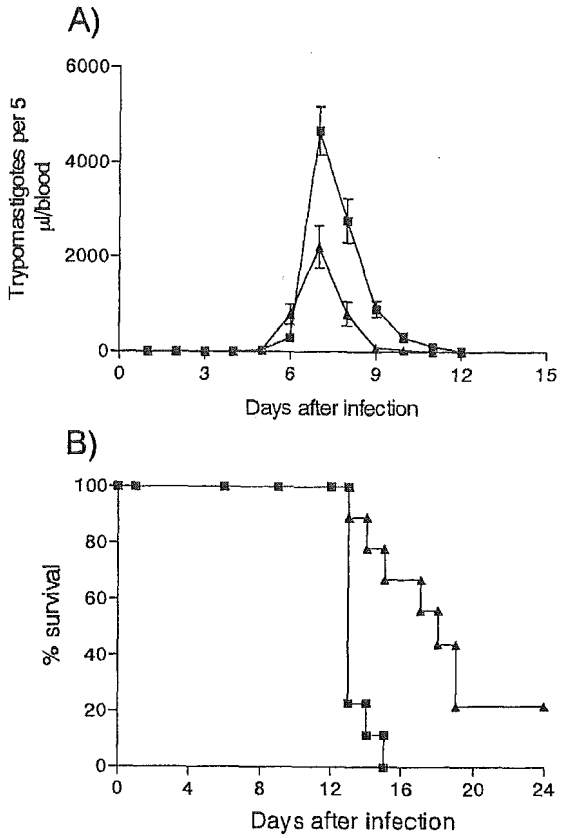

Fig. 1. Blood parasitemia (A) and lethality (B) during experimental *T. cruzi* infection in PAFR$^{-/-}$ and wild-type mice. PAFR$^{-/-}$ (squares) and wild-type (triangles) mice were infected with 5×10^3 trypomastigote forms of *T. cruzi* intraperitoneally. Results are shown as the mean ± S.E.M. of 10 mice per group in one of two independent experiments. The parasitemia and lethality curves of PAFR$^{-/-}$ and wild type were significantly different ($P < 0.01$).

3.2. Pathological alterations in T. cruzi-infected PAFR$^{-/-}$ mice

The morphological analysis of cardiac tissue of wild-type mice 10 and 15 d after infection showed few parasite nests scattered throughout the tissue (Fig. 2A). Parasite nests were already noticeable 10 d after infection only in PAFR$^{-/-}$ mice (Fig. 2A). Albeit in small quantities, heart sections of PAFR$^{-/-}$ mice had three-fold more parasite nests than those of wild-type mice 15 d after infection (Fig. 2A). Heart inflammation was characterized by the presence of multiple inflammatory focci composed mainly of mononuclear cells and a diffuse mononuclear cell infiltrate. The inflammatory infiltrate was already present on day 10 after infection but was more marked on day 15 in wild-type mice (Fig. 2B).

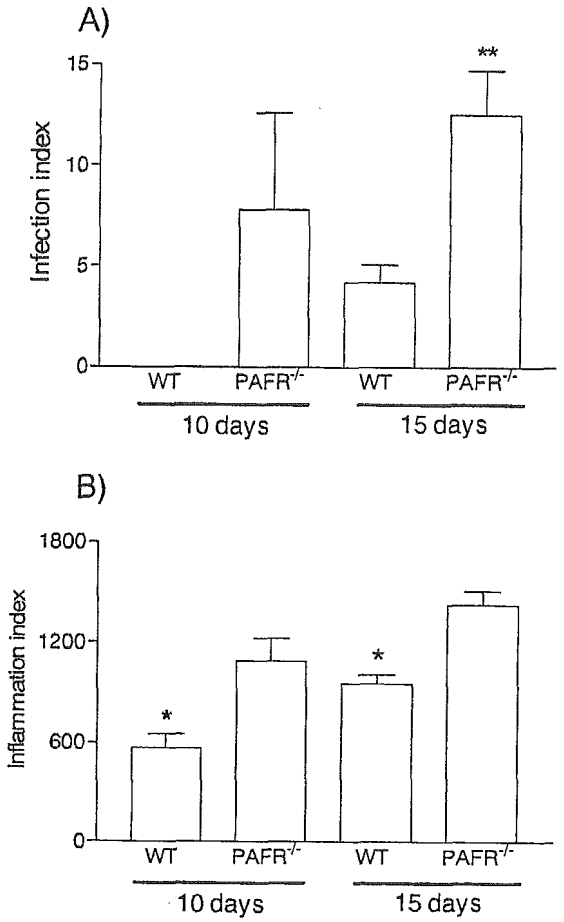

Fig. 2. Quantification of infection (A) and tissue inflammation (B) in $PAFR^{-/-}$ and wild-type mice. $PAFR^{-/-}$ and wild-type (WT) mice were infected with 5×10^3 trypomastigote forms of *T. cruzi* intraperitoneally, and inflammatory and parasitological indices were evaluated 10 and 15 d after infection. Results are shown as the mean ± S.E.M. of five mice per group. * and * * for $P < 0.05$ and 0.01, respectively, when compared with wild-type mice.

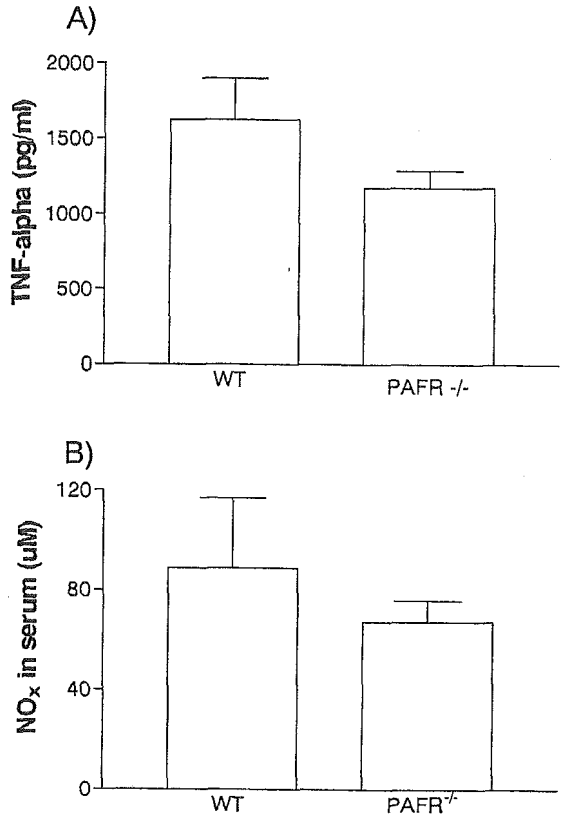

Fig. 3. Serum concentrations of TNF-α (A) and nitrate/nitrite (B) during experimental *T. cruzi* infection in $PAFR^{-/-}$ and wild-type mice. $PAFR^{-/-}$ and wild-type (WT) mice were infected with 5×10^3 trypomastigote forms of *T. cruzi* intraperitoneally, and serum concentrations of TNF-α and nitrate/nitrite (NO_x) were evaluated 10 d after infection. Results are shown as the mean ± S.E.M. of five mice per group.

Tissue inflammation in heart sections of $PAFR^{-/-}$ mice was of greater magnitude than that found in sections of hearts from wild-type mice (Fig. 2B).

3.3. *TNF-α, MCP-1, RANTES and IFN-γ synthesis in heart tissue* T. cruzi-*infected* $PAFR^{-/-}$ *mice*

The concentrations of TNF-α in serum of *T. cruzi*-infected wild-type and $PAFR^{-/-}$ mice are shown in Fig. 3A. Concentrations of TNF-α in serum of $PAFR^{-/-}$ mice were 28% lower than those of wild-type mice, but this difference failed to reach statistical significance ($P = 0.06$). TNF-α was not detected in serum of uninfected controls. Similarly, there was no significant difference between the concentration of nitrate and nitrite (NO_x) in serum samples of $PAFR^{-/-}$ and wild type after *T. cruzi* infection (Fig. 3B).

We have previously demonstrated the expression of TNF-α, RANTES, MCP-1 and IFN-γ mRNA in cardiac tissue of mice following *T. cruzi* infection [11]. Here, the concentrations of TNF-α, RANTES, MCP-1 and IFN-γ protein in heart tissues were detected using ELISA. Five days after infection, the concentration of TNF-α in infected mice was already elevated, and dropped to those found in uninfected controls by day 15 (Fig. 4A). The concentration of MCP-1 in infected wild-type mice was significantly greater than uninfected controls from day 5 and remained elevated throughout the 15-day observation period (Fig. 4B). The concentrations of TNF-α and MCP-1 in heart tissue of $PAFR^{-/-}$ mice were not different from those of infected wild-type mice (Fig. 4A,B). In contrast, there were some differences in the concentration of RANTES between the two groups. The RANTES concentration was higher than in uninfected controls only 10 d after infection, decreasing on day 15 (Fig. 4C). Ten days after infection RANTES protein expression was lower in $PAFR^{-/-}$ than wild type. However, there was a 40% increase in the levels of RANTES in $PAFR^{-/-}$ on day 15 (Fig. 4C). Concentrations of IFN-γ in heart tissue of infected wild-type mice were elevated from days 5 through 15 after infection, although there was a tendency for IFN-γ to drop on day 15 (Fig. 4D). The concentrations of IFN-γ in $PAFR^{-/-}$ mice were similar to those of wild-type controls at days 5 and 10 after infection and significantly greater on day 15 (Fig. 4D).

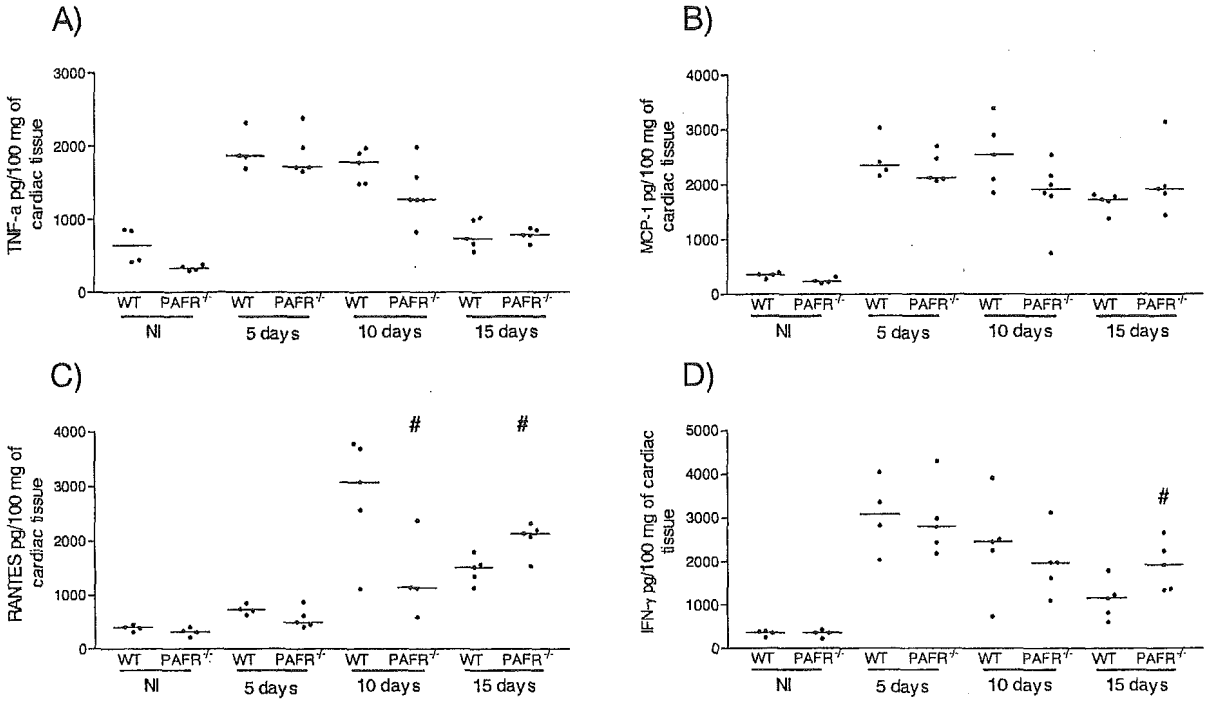

Fig. 4. Heart tissue concentrations of TNF-α (A), MCP-1 (B), RANTES (C) and IFN-γ (D) during experimental *T. cruzi* infection in PAFR$^{-/-}$ and wild-type mice. PAFR$^{-/-}$ and wild-type (WT) mice were infected with 5×10^3 trypomastigote forms of *T. cruzi* intraperitoneally, and heart tissue concentrations of TNF-α, MCP-1, RANTES and IFN-γ were evaluated 5, 10 and 15 d after infection. Each dot represents the result in single animals, and the bar, the mean value. # for $P < 0.05$ when compared with respective wild-type controls.

3.4. Titers of parasite-specific IgM

In order to evaluate whether the deficiency in PAFR would be accompanied by an altered ability of the host to mount an effective humoral response, parasite-specific IgM was measured after *T. cruzi* infection in wild-type and PAFR$^{-/-}$ mice. As clearly seen in Fig. 5, IgM was much greater in infected mice than in non-infected controls, but there was no significant alteration in the levels of this immunoglobulin between wild-type and PAFR$^{-/-}$ mice.

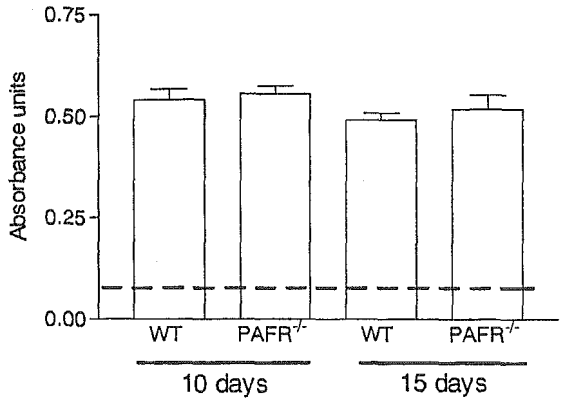

Fig. 5. Levels of parasite-specific IgM during experimental *T. cruzi* infection in PAFR$^{-/-}$ and wild-type mice. PAFR$^{-/-}$ and wild-type (WT) mice were infected with 5×10^3 trypomastigote forms of *T. cruzi* intraperitoneally, and serum concentration of parasite-specific IgM (1/100 dilution) was evaluated 10 and 15 d after infection. The dotted line across the graph represents background levels of IgM in non-infected mice. Results are mean ± S.E.M. of 3–4 mice per group.

3.5. Defective parasite uptake in PAFR$^{-/-}$ mice

The pretreatment of macrophages with PAF, LTB_4 and MCP-1 is accompanied by an early (within 2 h) increase in the uptake of parasites and a late (within 48 h) activation of inducible nitric oxide synthase (iNOS) and NO-dependent parasite killing [12,17,19]. In our experiments, pretreatment of macrophages derived from wild-type mice with PAF, LTB_4 or MCP-1 also induced a significant increase (1.5-fold increase of the basal uptake) in the early uptake of parasites (Fig. 6). In contrast, these agents failed to induce an increase in parasite uptake by macrophages derived from PAFR$^{-/-}$ mice (Fig. 6).

3.6. NO production by infected peritoneal macrophages

Pretreatment with PAFR antagonists partially inhibits the production of NO by infected macrophages activated with IFN-γ [12,19]. Uninfected macrophages from wild-type and PAFR$^{-/-}$ mice did not produce detectable concentrations of NO. When these cells were infected with *T. cruzi* in the presence of IFN-γ, macrophages from wild-type mice produced greater levels of NO than macrophages from PAFR$^{-/-}$ mice (infected wild-type macrophages + IFN-γ, 46.1 ± 3.0 μM of nitrite; infected PAFR$^{-/-}$ macrophages + IFN-γ, 21.6 ± 0.4 μM, $P < 0.05$).

4. Discussion

PAF, a membrane-derived phospholipid, is produced by a diversity of leukocytes and possesses widely recognized pro-

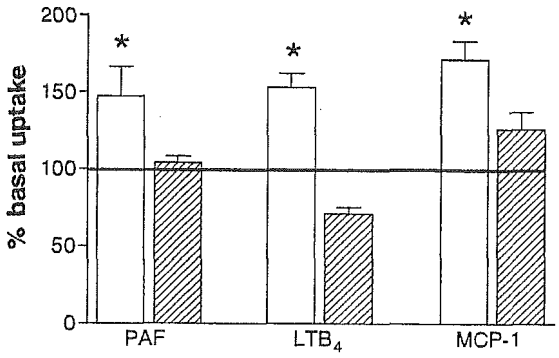

Fig. 6. *T. cruzi* trypomastigote uptake by macrophages in wild-type and PAFR$^{-/-}$ mice. Thyoglicolate-induced macrophages from wild-type (open bars) or PAFR$^{-/-}$ (hatched bars) mice were incubated with saline, PAF(1 μM), LTB_4 (0.1 μM) or MCP-1 (0.1 μM) for 10 min and then infected with *T. cruzi* in a 2:1 parasite:cell ratio. After 60 min, the number of parasites inside 200 macrophages was evaluated. The line across the graph represents basal uptake of parasites (27 ± 3 parasites in 200 saline-treated macrophages) in saline-treated macrophages. Results are shown as the % change from saline-treated animals, and are the mean ± S.E.M. of triplicate determinations in at least two experiments. * for $P < 0.05$ when compared with saline-treated macrophages.

inflammatory activities [14,15]. Here, we aimed at evaluating a pathophysiological role for PAF receptor during experimental *T. cruzi* infection by using animals genetically deficient for this receptor [20]. We evaluated potential differences in cardiac tissue inflammation and parasitism and in the production of cytokines between wild-type and PAFR$^{-/-}$ C57BL/6 mice.

Our results show that PAFR$^{-/-}$ mice are more susceptible to *T. cruzi* infection than their wild-type controls. Thus, PAFR$^{-/-}$ mice infected with *T. cruzi* had at least twice the amount of parasites in blood at the peak of parasitemia. The latter results are in agreement with our previous studies with PAFR antagonists [19]. Despite the paucity of amastigote nests in heart tissues of infected mice, the present study showed that there was greater tissue parasitism in PAFR$^{-/-}$ than in wild-type mice. Overall, the above results suggest that PAFR plays a relevant role in controlling parasitemia and tissue parasitism. More importantly, the increased tissue and blood parasitism and tissue inflammation in PAFR$^{-/-}$ animals was associated with lower survival following *T. cruzi* infection. The mechanism of infection-associated death was not investigated here, but it is clearly correlated with the inability of the murine host to deal with *T. cruzi* infection.

The production of IFN-γ by immune cells and the elevation of parasite-specific IgM are important immunological factors involved in host resistance to *T. cruzi* infection [5–8]. Thus, it was possible that a defective production of IFN-γ or IgM could account for the inability of PAFR$^{-/-}$ mice to deal with *T. cruzi* infection. However, our results suggest that this may not be the case, as the expression of IFN-γ in tissue and serum levels of IgM were similar in PAFR$^{-/-}$ and wild-type mice. Indeed, there was an even greater concentration of IFN-γ in heart tissue of PAFR$^{-/-}$ mice at the later stages of the infection. Whether this simply reflects (or causes) the greater presence of inflammatory cell infiltrate or whether the lack of PAFR facilitates the production of IFN-γ was not investigated here.

Several studies have demonstrated a role of PAF and its receptor for the migration of leukocytes during acute and chronic inflammation [15,24–26]. These actions of PAFR may be via a direct action of PAF on the leukocyte inducing its direct recruitment or via the production of PAF-induced chemoattractant mediators, such as LTB_4 or IL-8 [12,15,27]. In PAFR$^{-/-}$ mice, the greater intensity of tissue parasitism following *T. cruzi* infection was associated with a greater intensity of tissue inflammation. Thus, in contrast to other models of inflammation where PAF is relevant for the recruitment of inflammatory cells, it appears that activation of PAFR does not play a crucial role in the cascade of events that leads to the migration of leukocytes to heart tissue following *T. cruzi* infection in mice.

As tissue inflammation was enhanced in heart tissue of PAFR$^{-/-}$ mice, it was of interest to examine whether there was an increase in the tissue levels of chemoattractants thought to be relevant during experimental *T. cruzi* infection [3]. To this end, we measured the levels of the chemokines RANTES and MCP-1 in heart tissue of infected wild-type and PAFR$^{-/-}$ mice from 5 to 15 d after infection. Message RNA for both chemokines has been detected in *T. cruzi*-infected macrophages in vitro and in heart tissue following experimental infection in mice [11,17,28]. In addition, we have recently shown that MCP-1 release accounts for the ability of glycosylphosphatidylinositol-anchored mucin-like glycoproteins present on trypomastigotes to induce leukocyte recruitment in IFN-γ-primed mice [9]. MCP-1 was produced throughout the course of the infection, and no significant differences could be observed between wild-type and PAFR$^{-/-}$ mice. There was also significant expression of RANTES, especially after the 10th day of infection. In PAFR$^{-/-}$ mice, the levels of RANTES were lower than in controls on day 10 and higher on day 15. As heart tissue inflammation in PAFR$^{-/-}$ mice was already greater than controls on day 10, it is unlikely that RANTES would explain the greater tissue inflammation observed in these animals. However, the elevated levels of this chemokine in the later stages of infection (day 15) could be a contributing factor to the greater infiltration of leukocytes at a later stage. Interestingly, there was a good correlation between the expression of RANTES and IFN-γ in heart tissue in wild-type and PAFR$^{-/-}$ mice. In the latter group of animals, the increase in RANTES on day 15 above levels in infected wild-type mice was mirrored by an increased expression of IFN-γ. This is in agreement with our previous studies and suggestion that IFN-γ is a major regulator of RANTES and other chemokines during experimental *T. cruzi* pathology [3,11].

As inhibition of chemoattractant production and the influx of leukocytes did not appear to account for the worsening of experimental *T. cruzi* infection, we then evaluated whether the activation of PAFR was relevant for the production of TNF-α and NO, as we have previously demonstrated in vitro [12,19]. The concentration of NO_2/NO_3 in plasma of infected

wild-type and PAFR$^{-/-}$ mice was not significantly different. Similarly, there was no marked difference in concentration of TNF-α in plasma of PAFR$^{-/-}$ and wild-type mice. High levels of TNF-α were measured in heart tissue from the 5th to the 15th day of infection, in agreement with the ability of infected macrophages and cardiomyocytes to produced this cytokine [29]. Again, no differences were observed between wild-type and PAFR$^{-/-}$ mice. Thus, whereas PAFR may be relevant for the ability of infected macrophages to produce TNF-α in vitro, this receptor does not have any marked influence on the production of TNF-α when evaluated in the whole extract of the heart or in plasma.

The addition of chemoattractant mediators—including PAF, LTB_4 and MCP-1—to *T. cruzi*-infected peritoneal-derived macrophages induced the production of NO and NO-dependent killing [12,17,19]. NO production was greatly associated with an early increase in parasite uptake and a late activation of iNOS [12,17,19]. Preliminary studies from our laboratory suggest that chemoattractant-induced increase in parasite uptake appears to be secondary to the ability of these molecules to induce the phagocytosis of the parasite by macrophages (Santana et al., in preparation). Thus, whereas basal uptake of *T. cruzi* by macrophages was largely phagocytosis independent, chemoattractants enhanced parasite uptake through a mechanism suppressed by drugs that prevented phagocytosis. Importantly, the enhanced uptake of *T. cruzi* by macrophages was accompanied by enhanced NO production and NO-dependent killing [12,17,19]. Here, pretreatment of macrophages with PAF, LTB_4 or MCP-1 enhanced parasite uptake in wild-type but not in PAFR$^{-/-}$ mice. Of interest, PAF may not only act on surface receptors but also on nuclear PAFR to induce gene transcription and leukocyte activation [30], suggesting that measurement of PAF on supernatants is not useful, especially when there is a marked functional phenotype induced by PAFR antagonists or in gene-deficient mice. This is a situation similar to the necessary role of PAFR for the ability of neutrophils to phagocytose zymosan [27]. Overall, these results argue for an important role of PAFR in mediating uptake of *T. cruzi* parasites, possibly via facilitation of the expression of integrins [27] and phagocytosis. As enhanced early *T. cruzi* uptake is associated with enhanced NO-dependent killing at a later stage, it is possible that the greater tissue and blood parasitism observed in PAFR$^{-/-}$ mice may be secondary to the inability of tissue macrophages to deal with *T. cruzi* infection in vivo. In addition, IFN-γ-induced NO production was also partially dependent on the activation of PAFR, as demonstrated by experiments with PAFR antagonists [12,19] and PAFR$^{-/-}$ mice (shown here).

Thus, a situation may arise where, although present in sufficient numbers, macrophages may be unable to deal with infection, as they are not capable of phagocytosing and do not produce the necessary molecules, such as NO, to kill the parasite. The reason why macrophages treated with PAFR antagonists or those derived from PAFR$^{-/-}$ mice have defective NO production in the presence of IFN-γ is unknown. Nevertheless, our data suggest that the role of PAF during *T. cruzi* infection may stem from the role of this mediator in promoting phagocytosis of the parasite particle and subsequent production of effector molecules, such as NO. Further studies are necessary to evaluate the role of this lipid mediator for *T. cruzi* in other species and in humans.

Acknowledgements

This work was supported by Fundação Amparo a Pesquisas do Estado de Minas Gerais (FAPEMIG), Comissão Aperfeiçoamento Pessoal Ensino Superior (CAPES) and Conselho Nacional Desenvolvimento Científico de Tecnológico (CNPq). We are grateful to Dr. Fernando Cunha for performing the nitrate measurements and Dr. Elizabeth Camargos for helping with the morphometric analysis.

References

[1] J.C. Dias, Chagas'disease. Epidemiology and prevention, Arq. Bras. Cardiol. 63 (1994) 451–455.

[2] G.F. Mendez, M.R. Cowie, The epidemiological features of heart failure in developing countries: a review of the literature, Int. J. Cardiol. 80 (2001) 213–219.

[3] M.M. Teixeira, R.T. Gazzinelli, J.S. Silva, Chemokines, inflammation and *Trypanosoma cruzi* infection, Trends Parasitol 18 (2002) 262–265.

[4] M.M. Teixeira, I.C. Almeida, R.T. Gazzinelli, Introduction: innate recognition of bacteria and protozoan parasites, Microb. Infect. 4 (2002) 883–886.

[5] D.M. Engman, J.S. Leon, Pathogenesis of Chagas disease heart disease: role of autoimmunity, Acta Trop. 81 (2002) 123–132.

[6] M.B. Soares, L. Pontes-De-Carvalho, R. Ribeiro-Dos-Santos, The pathogenesis of Chagas' disease: when autoimmune and parasite-specific immune responses meet, An. Acad. Bras. Cienc. 73 (2001) 547–559.

[7] L. Pontes-de-Carvalho, C.C. Santana, M.B. Soares, G.G. Oliveira, E. Cunha-Neto, R. Ribeiro-Dos-Santos, Experimental chronic Chagas' disease myocarditis is an autoimmune disease preventable by induction of immunological tolerance to myocardial antigens, J. Autoimmun. 18 (2002) 131–138.

[8] Z. Brener, R.T. Gazzinelli, Immunological control of *Trypanosoma cruzi* infection and pathogenesis of Chagas' disease, Int. Arch. Allergy Immunol. 114 (1997) 103–110.

[9] P.S. Coelho, A. Klein, A. Talvani, S.F. Coutinho, O. Takeuchi, S. Akira, J.S. Silva, H. Canizzarro, R.T. Gazzinelli, M.M. Teixeira, Glycosylphosphatidylinositol-anchored mucin-like glycoproteins isolated from *Trypanosoma cruzi* trypamastigotes induce in vivo leukocyte recruitment dependent on MCP-1 production by IFN-γ-primed-macrophages, J. Leuk. Biol. 71 (2002) 837–844.

[10] P.V. dos Santos, E. Roffe, H.C. Santiago, R.A. Torres, A.P. Marino, C.N. Paiva, A.A. Silva, R.T. Gazzinelli, J. Lannes-Vieira, Prevalence of CD8 (+) alpha beta T cells in *Trypanosoma cruzi*-elicited myocarditis is associated with acquisition of CD62L (low) LFA-1 (high) VLA-4 (high) activation phenotype and expression of IFN-gamma-inducible adhesion and chemoattractant molecules, Microb. Infect. 3 (2001) 971–984.

[11] A. Talvani, C.S. Ribeiro, J.C.S. Aliberti, V. Michailowsky, P.V. Santos, S.M. Murta, A.J. Romanha, I.C. Almeida, J. Farber, J. Lannes-Vieira, J.S. Silva, R.T. Gazzinelli, Kinetics of cytokine gene expression in experimental chagasic cardiomyopathy: tissue parasitism and endogenous IFN-gamma as important determinants of chemokine mRNAs expression during infection with *Trypanosoma cruzi*, Microb. Infect. 2 (2000) 851–866.

[12] A. Talvani, F.S. Machado, G. Santana, A. Klein, L.S. Barcelos, J.S. Silva, M.M. Teixeira, Leukotriene B_4 induces nitric oxide synthesis in *Trypanosoma cruzi*-infected murine macrophages and mediates resistance to infection, Infect. Immun. 70 (2002) 4247–4253.

[13] F. Villalta, Y. Zhang, K. Bibb, J.C. Kappes, M.F. Lima, The cysteine–cysteine family of chemokines RANTES, MIP-1 alpha and MIP-1 beta induce trypanocidal activity in human macrophages via nitric oxide, Infect. Immun. 66 (1998) 4690–4695.

[14] P. Braquet, L. Touqui, T.Y. Shen, B.B. Vargaftig, Perspectives in platelet-activating factor research, Pharmacol. Rev. 39 (1987) 97–145.

[15] G. Montrucchio, G. Alloatti, G. Camussi, Role of platelet-activating factor in vascular cardiovascular pathophysiology, Physiol. Rev. 80 (2000) 1669–1699.

[16] A. Klein, V. Pinho, A.L. Alessandrini, T. Shimizu, S. Ishii, M.M. Teixeira, Platelet-activating factor drives eotaxin production in an allergic pleurisy in mice, Br. J. Pharmacol. 135 (2002) 1213–1218.

[17] J.C.S. Aliberti, F.S. Machado, J.T. Souto, A.P. Campanelli, M.M. Teixeira, R.T. Gazzinelli, J.S. Silva, β-chemokines enhance parasite uptake and promote nitric oxide-dependent microbiostatic activity in murine inflammatory macrophages infected with *Trypanosoma cruzi*, Infect. Immun. 67 (1999) 4819–4826.

[18] G.A. Martins, L.Q. Vieira, F.Q. Cunha, J.S. Silva, Gamma Interferon modulates CD95 (Fas) and CD95 ligand (Fas-L) expression and nitric oxide-induced apoptosis during the acute phase of *Trypanosoma cruzi* infection: a possible role in immune response control, Infect. Immun. 67 (1999) 3864–3871.

[19] J.C.S. Aliberti, F.S. Machado, R.T. Gazzinelli, M.M. Teixeira, J.S. Silva, Platelet-activating factor induces nitric oxide synthesis in *Trypanosoma cruzi*-infected macrophages and mediates resistance to parasite infection in mice, Infect. Immun. 67 (1999b) 2810–2814.

[20] S. Ishii, T. Shimizu, Platelet-activating factor (PAF) receptor and genetically engineered PAF receptor mutant mice, Prog. Lipid. Res. 39 (2000) 41–82.

[21] R.C. Melo, Z. Brener, Tissue tropism of different *Trypanosoma cruzi* strains, J. Parasitol. 64 (1978) 475–482.

[22] G.N.R. Vespa, F.Q. Cunha, J.S. Silva, Nitric oxide is involved in control of *Trypanosoma cruzi*-induced parasitemia and directly kills the parasite in vitro, Infect. Immun. 62 (1994) 5177–5182.

[23] B.M. Tavares-Murta, M. Zaparoli, R.B. Ferreira, M.L. Silva-Vergara, C.H. Oliveira, E.F. Murta, S.H. Ferreira, F.Q. Cunha, Failure of neutrophil chemotactic function in septic patients, Crit. Care Med. 30 (2002) 1056–1061.

[24] J.R. Jackson, B. Bolognese, C.A. Mangar, W.C. Hubbard, L.A. Marshall, J.D. Winkler, The role of platelet activating factor and other lipid mediators in inflammatory angiogenesis, Biochim. Biophys. Acta 1392 (1998) 145–152.

[25] Z. Honda, S. Ishii, T. Shimizu, Platelet-activating factor receptor, J. Biochem. 131 (2002) 773–779.

[26] D.G. Souza, D.C. Cara, G.D. Cassali, S.F. Coutinho, M.R. Silveira, S.P. Andrade, S. Poole, M.M. Teixeira, Effects of the PAF receptor antagonist UK74505 on local and remote reperfusion injuries following ischemia of the superior mesenteric artery in the rat, Br. J. Pharmacol. 131 (2000) 1800–1808.

[27] B.T. Au, M.M. Teixeira, P.D. Collins, T.J. Williams, Blockade of PAF receptors controls IL-8 production by regulating the activation of neutrophil CD11/CD18, Eur. J. Pharmacol. 425 (2001) 65–71.

[28] J.C.S. Aliberti, J.T. Souto, A.P.M. Marino, J. Lannes-Vieira, M.M. Teixeira, J. Farber, R.T. Gazzinelli, J.S. Silva, Modulation of chemokine production and inflammatory responses in interferon-γ and tumor necrosis factor-R1-deficient mice during *Trypanosoma cruzi* infection, Am. J. Pathol. 158 (2001) 1433–1440.

[29] F.S. Machado, G.A. Martins, J.C.S. Aliberti, F.L.A.C. Mestriner, F.Q. Cunha, J.S. Silva, *Trypanosoma cruzi*-infected cardiomyocytes produce chemokines and cytokines that trigger potent nitric oxide-dependent Trypanocidal activity, Circulation 102 (2000) 3003–3008.

[30] A.M. Marrache, F. Gobeil Jr., S.G. Bernier, J. Stankova, M. Rola-Pleszczynski, S. Choufani, G. Bkaily, A. Bourdeau, M.G. Sirois, A. Vazquez-Tello, L. Fan, J.S. Joyal, J.G. Filep, D.R. Varma, A. Ribeiro-Da-Silva, S. Chemtob, Proinflammatory gene induction by platelet-activating factor mediated via its cognate nuclear receptor, J. Immunol. 169 (2002) 6474–6481.

Preparation of 7-Substituted Ginkgolide Derivatives: Potent Platelet Activating Factor (PAF) Receptor Antagonists

Stine Byskov Vogensen,[†,§] Kristian Strømgaard,[†,§] Hideo Shindou,[‡] Stanislav Jaracz,[†] Makiko Suehiro,[†] Satoshi Ishii,[‡] Takao Shimizu,[‡] and Koji Nakanishi[†,*]

Department of Chemistry, Columbia University, 3000 Broadway, New York, New York 10027, Department of Biochemistry and Molecular Biology, Faculty of Medicine, The University of Tokyo, Hongo 7-3-1, Bunkyo-ku, Tokyo 113-0033, Japan, and CREST of Japan Science and Technology Corp., Tokyo 113-0033, Japan

Received September 12, 2002

Ginkgolides are structurally unique constituents of *Ginkgo biloba* extracts and are known antagonists of the platelet-activating factor (PAF) receptor. Ginkgolide C is 25-fold less potent than ginkgolide B as a PAF receptor antagonist, due to the presence of the 7β-OH. Recently, we found that 7α-fluoro ginkgolide B was equipotent to ginkgolide B underlining the critical importance of the 7-position of ginkgolides for PAF receptor activity. Herein we describe the synthesis of a series of ginkgolide B derivatives with modifications at the 7-position and the pharmacological evaluation of these derivatives as assayed by cloned PAF receptors. In two cases nucleophilic attack on a 7β-*O*-triflate ginkgolide B did not lead to the expected products, but gave rise to two unprecedented ginkgolide derivatives, one with a novel rearranged skeleton. Furthermore, standard reduction of 7α-azido ginkgolide B did not give the expected primary amine, but instead yielded alkylated amines depending on the solvent employed. Pharmacological testing with cloned PAF receptors showed that ginkgolides with 7α-substitutents had increased affinity compared to 7β-substituents, in particular 7α-chloro ginkgolide B, the most potent nonaromatic ginkgolide derivative described to date with a K_i value of 110 nM.

Introduction

Ginkgo biloba L., the last surviving member of a family of trees (*Ginkgoaceae*) that appeared more than 250 million years ago, has been mentioned in the Chinese Materia Medica for more than 2500 years.[1] A standardized *G. biloba* extract (EGb 761) containing terpene trilactones (5−7%) and flavonoids (22−24%) has demonstrated neuromodulatory properties.[2,3] Several clinical studies using EGb 761 have reported positive effects on various neurodegenerative diseases, including Alzheimer's disease,[4−6] and recent studies on healthy volunteers have shown positive effects of EGb 761 on short-term working memory.[7,8]

A number of *G. biloba* constituents have been isolated, including the unique terpene trilactones, i.e., ginkgolides A, B, C, J and M and bilobalide.[9−12] Ginkgolides are diterpenes with a cage skeleton consisting of six five-membered rings, the difference between the five ginkgolides being in the variation in the number and positions of hydroxyl groups on the spirononane framework. Although the molecular basis for the action of *G. biloba* terpene trilactone constituents in the central nervous system (CNS) is only poorly understood, it is known that ginkgolides, particularly ginkgolide B (GB, **1**, Figure 1), is a potent in vitro antagonist of the platelet-activating factor receptor (PAFR).[13,14] The PAFR is a potential target for neurodegenerative diseases,[15] while PAF (1-*O*-alkyl-2-acetyl-*sn*-glycero-3-phosphocholine) has been suggested as a retrograde messenger in long-term potentiation (LTP),[16] thus indicating the importance of the PAFR as a target for ginkgolides.

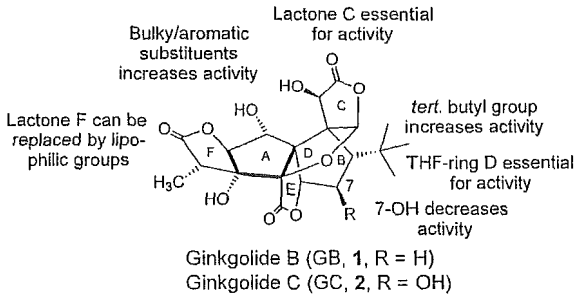

Figure 1. Summary of structure−activity relationship (SAR) studies of ginkgolides as PAFR antagonists. GB (**1**) is ca. 25-fold more potent than GC (**2**).

Structure−activity relationship (SAR) studies of ginkgolides on the PAFR have primarily focused on GB (**1**) (Figure 1) derivatives[17−21] as outlined in Figure 1, e.g., the importance of lactones and the *tert*-butyl group has been investigated, whereas the effect of stereochemistry of hydroxyl groups remains to be examined. Ginkgolide C (GC, **2**, Figure 1), having a hydroxyl group at C-7, is significantly less potent than GB (**1**),[22] which has been explained by the hydrophilic 7β-OH of GC (**2**) being next to the lipophilic *tert*-butyl group, which is believed to interact with a lipophilic pocket in the PAFR.[14] Moreover, substitution at 7-OH further decreases antagonistic activity, as demonstrated by 7-*O*-(4-methylphenyl)-GB that was devoid of PAFR activity[23]

* To whom correspondence should be addressed. Phone: +1 212 854 2169. Fax: +1 212 932 8273. E-mail: kn5@columbia.edu.
† Department of Chemistry, Columbia University.
‡ Department of Biochemistry and Molecular Biology, The University of Tokyo and CREST of Japan Science and Technology Corp.
§ Present address: Department of Medicinal Chemistry, Pharmaceutical University of Denmark, DK-2100 Copenhagen, Denmark.

10.1021/jm0203985 CCC: $25.00
Published on Web 01/21/2003

Scheme 1[a]

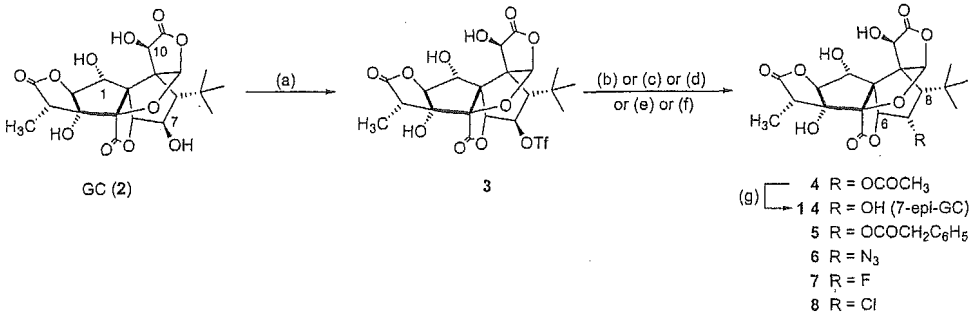

[a] Reagents: (a) Tf_2O, pyridine, CH_2Cl_2; (b) $NaOCOCH_3$, DMSO; (c) $NaOCOCH_2C_6H_5$, DMSO; (d) NaN_3, DMSO; (e) TBAF, CH_3CN; (f) TBACl, CH_3CN; (g) 2 N NaOH.

Scheme 2[a]

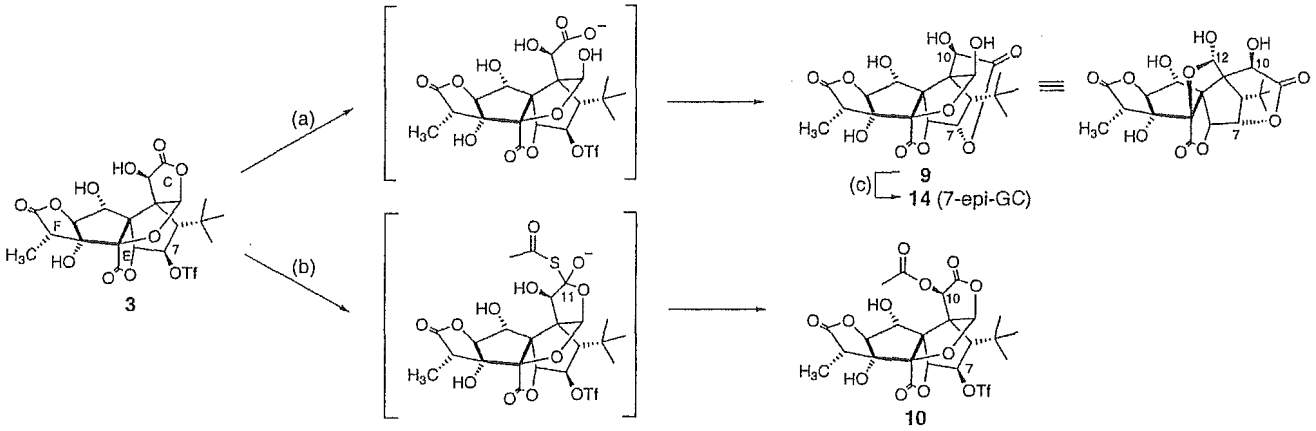

[a] Reagents: (a) MeOH, 2,6-lutidine; (b) $KSCOCH_3$, DMF; (c) 1 M NaOH, acidic workup.

and a 7-*O*-dansyl-GB derivative was also less potent than the parent compound.[22]

Preliminary studies showed that 7α-F-GB was equipotent to GB and 15-fold more potent as a PAFR antagonist as compared to GC (**2**),[24] despite the fact that fluorine is sterically equivalent to OH and more polar than hydrogen.[25] Since configuration of the fluorine atom is α, whereas that of the 7-hydroxyl in GC (**2**) is β, it is not clear whether this difference in activity is due to changes in stereochemistry, steric effects, or electronic effects. In the following, we describe a series of ginkgolide derivatives with variation at the critical 7-position and the assessment of these derivatives for their ability to displace radioligand binding to cloned PAFR.

Results

Synthesis. For the synthesis of derivatives with variation at C-7, a crucial intermediate was 7β-OTf-GB (**3**). GC (**2**) reacted with remarkable selectivity at 7-OH with trifluoromethanesulfonic (Tf) anhydride giving **3** in very high yield, with no reactions occurring at other hydroxyl groups.[26] This selectivity is noteworthy, as 10-OH, and in some cases 1-OH, of GC (**2**) is generally the more reactive hydroxyl group,[19,21] although we recently observed higher reactivity of 7-OH when acetylation was performed under strong acidic conditions.[27]

7β-OTf-GB (**3**) was reacted with various nucleophiles as depicted in Scheme 1 to give derivatives **4**–**8**. The inverted configuration at C-7 was reflected by considerable changes in coupling constants in ^1H NMR spectra, i.e., $^3J_{7,8}$ and $^3J_{6,7}$ are 12 and 4 Hz in GC (**2**), whereas they are 3–5 Hz and ca. 0 Hz, respectively, when the configuration at C-7 is inverted. The reactions shown in Scheme 1 generally proceeded in good yield, but in several other cases the nucleophilic substitution did not proceed as expected. When reacting with a soft nucleophile such as NaSCN, only starting material was recovered. Increase in the basicity of the nucleophiles, as in NaCN and aliphatic amines, resulted in a complex mixture of products, probably due to reaction at C-11, as previously described.[28] In addition to the presence of multiple electrophilic sites in **3** it is believed that the steric hindrance of the bulky *tert*-butyl group, which is in close proximity to the reaction site, is responsible for lack of reaction. This assumption is corroborated by reaction of **3** with halogens; incorporation of fluorine (7α-F-GB, **7**) proceeded in high yield and chlorine (7α-Cl-GB, **8**) in slightly lower yield, whereas the larger bromine was introduced in trace amounts only, while no iodine product could be detected. These results were not affected by changing the solvent or the halide counterion.

Steric hindrance may also be the prerequisite for two remarkable products arising from reaction of triflate **3** with MeOH and $NaSCOCH_3$, respectively (Scheme 2). In the former case **3** was dissolved in MeOH and 2,6-lutidine and reacted for 3 days at 70 °C expecting to provide 7α-OMe-GB; instead a new product with a molecular weight similar to GC (**2**), but with a different ^1H NMR spectrum, was obtained. Extensive NMR studies revealed a new relactonized structure, neo-

Table 1. Reduction of 7α-N_3-GC (**6**) in Different Solvents

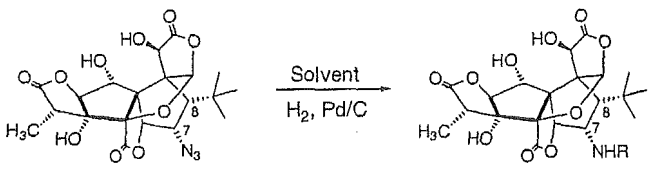

6

compound	solvent	R	yield (%)[a]
11	MeOH	CH_3	95
12	EtOH	CH_2CH_3	68
13	THF	H	98

[a] Isolated yield (after flash chromatography).

ginkgolide C (**9**) (Scheme 2), arising from opening of lactone C, followed by displacement of the triflate group. The structure of this compound **9** with a new rearranged ginkgolide skeleton not encountered earlier was determined by high resolution mass spectrometry, rotating frame nuclear Overhauser and exchange spectroscopy (ROESY), correlation spectroscopy (COSY), and heteronuclear single-quantum coherence (HSQC) NMR experiments (see Supporting Information). Moreover, treatment of neoginkgolide C (**9**) with 1 M NaOH followed by acidic workup resulted in a clean conversion to the thermodynamically more favorable 7-epi-GC (**14**). The reaction between triflate **3** and $NaSCOCH_3$ did not give the expected 7α-$SCOCH_3$-GB, but instead the 10-acetate, while the 7-triflate group remained intact to give **10** (Scheme 2). This product might arise from a reaction by thioacetate at C-11, followed by a transfer of the acetate to 10-OH, tautomerization to thionic acid, and relactonization to give the final product (Scheme 2).

Another interesting feature was the reduction of azide **6** using Pd/C in MeOH under hydrogen. The reaction did not provide the expected amine, but instead gave *N*-methylamine **11** in quantitative yield (Table 1). To investigate this further, the reaction was carried out in EtOH, which gave *N*-ethylamine **12** as the major product. The desired primary amine **13** was obtained when THF was used as solvent (Table 1). This intriguing reaction might provide a convenient way to convert azides directly into various alkylamines, an aspect which is under further investigation.

For the synthesis of 7-epi-GC (**14**) (Scheme 1) various approaches were attempted; GC (**2**) and 4-nitrobenzoic acid were treated with diethyl azodicarboxylate (DEAD) and Ph_3P in a Mitsunobu reaction, but no reaction was observed. Instead, 7β-OTf-GB (**3**) was reacted with KNO_2 and 18-crown-6 ether in a reaction that could potentially lead to 7-epi-GC (**14**) directly from **3**,[29] but only starting material was recovered. Instead, the inversion of 7-OH of GC (**2**) was accomplished using acetate as the nucleophile, followed by basic hydrolysis of the acetate. Acetylation of 7β-OTf-GB (**3**) was achieved by reaction with NaOAc; attempts to use the more reactive CsOAc led to decomposition of **3**, while using $CsOCCF_3$ did not lead to any reaction. The hydrolysis was accomplished by treating **4** with 2 N NaOH to give 7-epi-GC (**14**) in 95% yield (Scheme 1).

Since the importance of sterochemistry at 1- and 10-OH of ginkgolides for PAFR activity is not known, we were interested in preparing 1- and 10-OTf derivatives of GB. However, reaction of GB (**1**) with Tf anhydride failed to give any desired product, and instead several elimination products were obtained, originating from elimination of 3-OH, as well as 1-OH. Similarly, reaction of GB (**2**) with *p*-toluenesulfonyl (tosyl) chloride gave two main products, both with a tosyl group at 10-OH, and elimination of either 3-OH or both 3- and 1-OH, respectively.

To further investigate the importance of stereochemistry at C-7, we planned a series of corresponding 7β-substituted derivatives. Thus 7-epi-GC (**14**) was reacted with Tf anhydride, but only starting material was recovered. This lack of reaction is most likely due to a change in steric environment of 7α-OH, relative to 7β-OH, due to the *tert*-butyl group.

Finally, the observation that an aromatic substituent at 10-OH of GB (**1**) and GC (**2**) increases the antagonistic effect at PAFR[19,21,22] led us to investigate whether a similar increase would be observed for 7α-GB derivatives. Benzylated derivatives **15**–**18** (Table 3) were therefore prepared, following previously described procedures.[19,21]

Pharmacology. Derivatives **4**–**9** and **11**–**18** were tested for their ability to displace [^{3}H]-WEB 2086 binding to cloned PAFR (Tables 2 and 3) using membrane fractions from hearts and skeletal muscles of PAFR transgenic mice, as previously described.[30] In these fractions, GB (**1**) had a K_i value of 0.88 μM, thus being similar to the previously determined K_i value of 0.56 μM.[22]

Derivatives with 7α-substituents were all more potent than GC (**2**) (Table 2), but within this group of compounds there were marked differences; 7α-OAc, 7α-OCOBn, 7α-OH, and 7α-NH_2 ginkgolide B derivatives all had K_i values between 2.4 and 7.8 μM, thus being slightly more potent than GC (**2**), but still significantly less potent than GB (**1**). Compounds **6**, **7**, **11**, and **12** with 7α-N_3, 7α-F, 7α-NHMe, and 7α-NHEt substituents, respectively, were equipotent to GB (**2**) with K_i values in the range of 0.55–1.62 μM. Finally, 7α-chloro ginkgolide B (**8**) was the most potent compound in this series with a K_i value of 0.11 μM, thus being the most potent nonaromatic ginkgolide derivative described.

The relactonized compound **9** (Scheme 2) was also tested for binding to PAFR and was found to be essentially inactive with a K_i value > 40 μM. Benzyl derivatives were investigated as well (Table 3), and as expected a 10-*O*-benzyl group significantly improved the affinity for PAFR. Compounds **15** and **17** were the most potent with K_i values of 0.12 and 0.10 μM, respectively, while 10-*O*-benzyl-GC (**16**) and 10-*O*-benzyl-7-epi-GC (**18**) were slightly less potent with K_i values of 1.67 and 0.60 μM, respectively.

Discussion

Herein the effect of modification of the C-7 position of ginkgolides has been investigated by synthesis of 15 analogues (**4**–**18**), which have been prepared from native ginkgolides GB (**1**) and GC (**2**) and evaluated with the cloned PAFR.

The derivatives with 7α-substituents were prepared by nucleophilic substitution of 7β-OTf-GB (**3**), but in

Table 2. K_i Values of Ginkgolide B (**1**) and C (**2**), and 7-Epi Derivatives

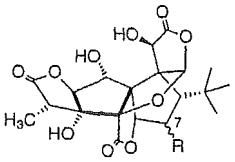

compound	R	K_i (μM)[a]	compound	R	K_i (μM)[a]
GB (1)	H	0.88	7α-F-GB (**7**)	α-F	0.99
GC (2)	β-OH	12.6[b]	7α-Cl-GB (**8**)	α-Cl	0.11
7α-OAc-GB (**4**)	α-OAc	7.84	7α-NHMe-GB (**11**)	α-NHMe	0.61
7-epi-GC (**14**)	α-OH	4.26	7α-NHEt-GB (**12**)	α-NHEt	1.62
7α-$OCOCH_2Ph$-GB (**5**)	α-$OCOCH_2Ph$	2.40	7α-NH_2-GB (**13**)	α-NH_2	8.64
7α-N_3-GB (**6**)	α-N_3	0.55			

[a] Inhibition of [^{3}H]-WEB 2086 binding. Values are means of two independent experiments performed in triplicate. [b] Data from previous studies.[22]

Table 3. K_i Values of Benzylated Derivatives

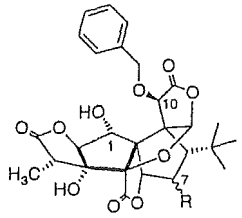

compound	R	K_i (μM)[a]
10-OBn-GB (**15**)	H	0.12
10-OBn-GC (**16**)	β-OH	1.67
10-OBn-7α-F-GB (**17**)	α-F	0.10
10-OBn-epi-GC (**18**)	α-OH	0.60

[a] Inhibition of [^{3}H]-WEB 2086 binding. Values are means of two independent experiments performed in triplicate.

several cases these reactions did not proceed as expected. Attempts to introduce larger halogens such as bromine and iodine, as well as other nucleophiles, failed. In the reaction between **3** and $NaSCOCH_3$, the 7-OTf group remained intact; instead the reaction presumably took place at C-11 of lactone C to give **10** (Scheme 2). Reaction of **3** with MeOH and 2,6-lutidine gave rise to neoginkgolide C (**9**) with a novel rearranged skeleton (Scheme 2). This compound had a K_i value > 40 μM, which is in agreement with previous studies which showed that modification of lactone C significantly reduced PAFR binding (Figure 1).[28]

During the reduction of azide **6** interesting observations were made; when carried out in MeOH this reaction did not give the expected primary amine **13**, but gave *N*-methylamine **11** instead and when carried out in EtOH the reduction gave *N*-ethylamine **12**. Besides being a potential novel procedure for a direct conversion of azides into alkylated amines, it also raises mechanistic considerations. Treatment of **13** with Pd/C in MeOH gave **11**, albeit in lower yield than starting from azide **6**, and with several side products. This implies that in the preparation of **11** and **12** the azide **6** is initially reduced to amine **13**, which then reacts instantly with the oxidized solvent to form an imine that is reduced to yield the products. Further studies are required to confirm this pathway, as well as the generality of this reaction. These studies are ongoing in our laboratory.

The prepared derivatives were tested for binding to cloned PAFR (Tables 2 and 3). It was observed that 7α-derivatives were slightly more potent than the 7β-derivatives, as GC (**2**) had a K_i value of 12.6 μM, while for 7-epi-GC (**14**), the K_i is 4.26 μM. Likewise 7α-OAc-GB (**4**) had a K_i of 7.84 μM, while 7β-OAc-GB (i.e., 7-OAc-GC) had been shown to have low potency comparable to that of GC (**2**).[27] Furthermore, the 7α derivative **5** is a reasonable potent PAFR antagonist with a K_i value of 2.40 μM (Table 2) in contrast to 7β-*O*-(4-methylphenyl)-GB, which is devoid of PAFR activity.[23] However as these differences are relatively small, the C-7 configuration seems to play only a minor role for PAFR antagonistic activity.

The nature of the 7α-substituent, on the other hand, had a major impact on the binding to PAFR. Introduction of azide and fluorine groups yielded compounds that were equipotent to GB (**1**) (Table 2), while introduction of a chlorine as in 7α-Cl-GB (**8**) leads to a dramatic increase in binding affinity. Thus **8** with K_i = 0.11 μM, was 115-fold more potent than GC (**2**) and 8-times more potent than GB (**1**), thereby being the most potent nonaromatic ginkgolide derivative described to date. It appears that polar groups that can form hydrogen bonds decrease activity, as seen in 7-epi-GC (**14**) and 7α-NH_2-GB (**13**), with a hydroxyl and a primary amino group, respectively, at C-7, both having binding affinities lower than GB. On the other hand, alkylation of **13** to give 7α-NHMe-GB (**11**) and 7α-NHEt-GB (**12**) led to significant increases in binding affinities, with K_i values of 0.61 μM and 1.62 μM, respectively. Rationalization of these trends requires further molecular mechanistic studies of the ginkgolide-PAFR interaction, which are ongoing in our laboratory.

Introduction of benzyl groups in the 10-OH position of ginkgolides is known to improve affinity for PAFR,[19,21,22] but whether this is true for 7α-substituted derivatives was not known. The affinities of 10-*O*-benzyl-7α-F-GB (**17**) and 10-*O*-benzyl-7-epi-GC (**18**) (Table 3) shows 10- and 7-fold improved affinity compared to their nonbenzylated derivatives. Thus 10-benzylation of 7α-substituted derivatives improves binding affinity as previously shown for other ginkgolide derivatives.

In conclusion we have synthesized several ginkgolide derivatives with modifications at C-7. These syntheses have led to several unexpected products such as **9** and **10**, as well as a potential novel procedure for a direct conversion of azides into alkylamines. Moreover, contrary to previous convictions, we have shown that